**DEMOCRATIC AND POPULAR REPUBLIC OF ALGERIA**

**MINISTRY OF HIGHER EDUCATION AND SCIENTIFIC RESEARCH**

**MOHAMED BOUDIAF UNIVERSITY - M'SILA**


**FACULTY OF TECHNOLOGY**

**DEPARTMENT OF ELECTRONICS**

**FIELD: Electronics**

**OPTION: Electronics of Embedded Systems**

**N°:**

**A dissertation submitted to obtain**

**Academic Master's degree**

**By:**

Ahmed Rafik ZOUAOUI

Rafik Abdelhak NADIR

**THEME**

# A Deep Learning Approach for Early Diagnosis of Alzheimer’s Disease using MRI Images

**Supervisor: Dr. BRIK Youcef**

**2021 /2022**

## Thanks

First and foremost, I am grateful to Allah for the good health and wellbeing that were necessary to complete this thesis.

I am extremely grateful to my supervisor, Dr. BRIK Yousef, for his invaluable advice, continuous support, and patience during my thesis writing. His immense knowledge and plentiful experience have encouraged me all the time in my academic research and daily life. I would also like to thank Dr. DJERIOUI Mohamed and Dr. ATTALLAH Bilal for their technical support in my study. Finally, I would also like to thank all the teachers of the electronic department for the quality of the training provided during my years of study.

## Dedication

I am dedicating this thesis to all Alzheimer’s patients, in particular my aunt's husband. Although he passed away two years ago due to Alzheimer's disease, might this work help to fight this disease.

I am dedicating this to my family, my mother, my father, and my two sisters. Thank you for having my back.

To all my friends and fellow students of the electronic class of 2022, in particular Haithem, Lahcen, and Nassim.

# Table of contents

# Figures list

# Tables list

# General Introduction

# General Introduction

On this day, at least 50 million individuals worldwide are estimated to be living with Alzheimer's disease or other forms of dementia. If no breakthroughs are made, rates might reach 152 million by 2050. Scientists do not yet fully comprehend what causes Alzheimer's disease in the majority of people. The causes are most likely a combination of age-related brain changes, as well as genetic, environmental, and lifestyle factors. The impact of any of these factors in increasing or decreasing the risk of Alzheimer's disease varies by individual.

Alzheimer's disease is a degenerative neurological disorder. It is classified by brain abnormalities such as amyloid plaques and neurofibrillary, or tau, tangles, which result in the death of neurons and their connections. These and other changes have an impact on a person's ability to remember and think, as well as their ability to live independently.

Alzheimer's is not triggered by old age, yet it is the most important recognized risk factor for the disease. After the age of 65, the number of people with Alzheimer's disease roughly doubles every 5 years. Alzheimer's disease affects almost one-third of all adults aged 85 and up. Scientists are learned how age-related brain changes might destroy neurons and alter other types of brain cells, contributing to Alzheimer's disease damage. These age-related changes include brain atrophy (shrinking), inflammation, vascular damage, the development of unstable chemicals known as free radicals, and the breakdown of energy production inside cells. Age is, however, only one risk factor for Alzheimer's disease. Many people live well into their 90s and beyond and never get dementia. Early detection of Alzheimer's disease is essential as a first step, and classification is necessary as a second phase for patients to receive the best possible treatment, or at least limit its rapid advance. Because MR imaging is one of the best ways to help and contribute to detecting it due to the high-quality pictures that it captures, and because there are numerous datasets of Alzheimer's disease, a system for the early detection and classification of Alzheimer's disease is expected.

Artificial intelligence, especially machine learning and deep learning techniques, has made a whole change in the medical world and helped many doctors solve huge health problems. Moreover, we can find some researchers and data scientists who created and developed some programs that trait images.

We can use transfer-learning techniques to implement the available pre-trained models, which will save a lot of time. When we say available, we mean that there are many models to

choose from. We chose two models for our research: VGG16 and MobileNetV2. Using the datasets collected from Kaggle, retrain the last layer of the model, which contains the classification classes, in our case, Alzheimer's disease, in the transfer learning technique. With MobileNtV2 and VGG16, we were able to obtain some outstanding results.

In the first chapter, we looked at the biomedical data that is currently available, with a focus on biomedical imaging. We have also looked deeper into artificial intelligence, machine learning, and deep learning to examine how they can help in healthcare.

We defined Alzheimer's disease in the second chapter, and then we discussed the relationship and importance of AI in the Alzheimer's disease fighting effort. We ended it up with a brief comparison with state-of-the-art approaches.

We outlined our system architecture and provided a brief explanation of the datasets, pre-processing techniques, and evaluation metrics used to assess the performance of the CNN models in the last chapter. Finally, we compared our model to models of transfer learning techniques and state-of-the-art approaches.

# Chapter I: Biomedical data and artificial intelligence

## I.1. INTRODUCTION

The application of engineering principles and design concepts to medicine and biology for the cause of healthcare is called biomedical engineering (e.g., diagnostic or therapeutic). This discipline creates a link between engineering and medicine by combining engineering's design and problem-solving skills with medical biology to enhance healthcare treatment, inclusive of diagnosis, monitoring, and therapy. A biomedical engineer's obligations additionally consist of the management of current medical equipment in hospitals at the same time as adhering to industry standards.

The increasing number of computer hardware and software applications in medicine and the digitization of health data are driving advances in the development and use of artificial intelligence in medicine [Wang, 2019]. This advance offers new opportunities and challenges, as well as the future direction of artificial intelligence in healthcare.

In this chapter, we will review the biomedical data available today and focus on biomedical images. We'll also dive deeper into artificial intelligence and see how it can play an important role in healthcare.

## I.2. BIOMEDICAL DATA

Biomedical data can be in various forms, obtained from various sources such as CT and MRI images; EEG signals; laboratory data from blood, and sample analysis; and clinical data of the patient.

### I.2.1. Different types of 2D biomedical data

#### I.2.1.1. X-Ray images

X-rays are high-energy electromagnetic radiation. They have energies ranging from about 200 eV to 1 MeV, which puts them between γ-rays and ultraviolet (UV) radiation in the electromagnetic spectrum [Suryanarayana, 1998].

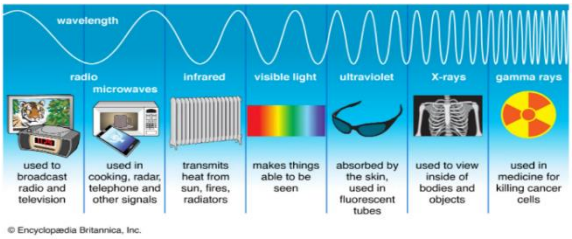


(a)

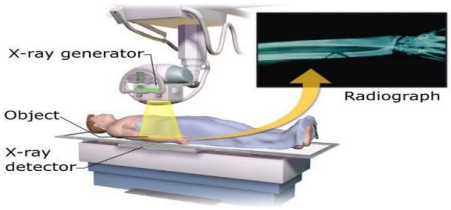


(b)

(c)

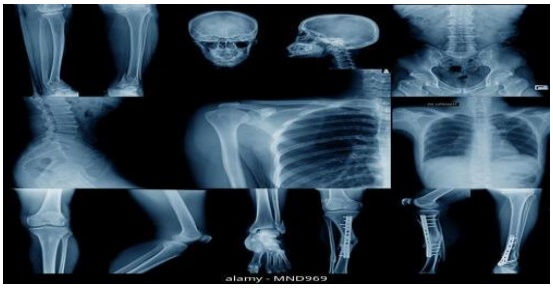


**Figure 1.** X-Ray Imaging a) Types of Electromagnetic Radiation and b) X-ray machines, and c) Collection of X-Rays Images for the human body.

### I.2.1.2. PET images

Positron Emission Tomography (PET) is a non-invasive nuclear medicine technique that allows for the quantitative measurement of physiological and pathological function via different radiopharmaceuticals. PET is a functional imaging tool that enables the tracing of blood flow and volume, glucose metabolism, oxygen, and drug efficacy. PET has enhanced diagnostics, particularly in the field of oncology, and has become a vital tool in research, facilitating additional insight into many neurological disorders, including dementias and psychiatric disorders. 18F-fluorodeoxyglucose (18F-FDG) is the most commonly used radiotracer diagnostically. However, there are several different radiotracers enabling the visualization of different biological processes [Brown, 2022].

**Figure 2.** PET Imaging a) Positron emission tomography (PET) scanner, and b) Positron emission tomography (PET) scan for the human brain.

### I.2.1.3. CT images

A CT scan is a diagnostic imaging procedure that uses X-rays and computer technology to produce images of the inside of the body. CT was firstly used for depicting the brain anatomy of a patient in 1971 in the UK.

CT is an important diagnostic tool, used to evaluate many medical conditions. In recent years, there have been several notable advances in CT technology that have already had or are expected to have significant clinical impact, including extreme multidetector CT, iterative reconstruction algorithms, dual-energy CT, cone-beam CT, handheld CT, and phase contrast CT [Ginat, 2014].

The high-resolution CT images allow the accurate separation of the various body compartments at the tissue/organ level, including adipose tissue, skeletal muscle, bones, and organs. The further ability of the imaging modality to differentiate the cortical from the trabecular bone and the visceral from the subcutaneous fat is of great value in clinical studies. CT can also give important information about the components of the subcutaneous adipose tissue and the muscle or liver fat infiltration. The efficient determination of the skeletal muscle attenuation and bone mineral density, related to metabolic disorders, is feasible with the help of CT data. The area and volume of each human body compartment may be estimated with high accuracy and reproducibility from CT scans. These estimations may be carried out using the methods of manual planimetry, semi-automatic segmentation of the tissue of interest, stereological point-counting approach, and geometrical models based on either linear or area measurements [Mazonakis, 2016].

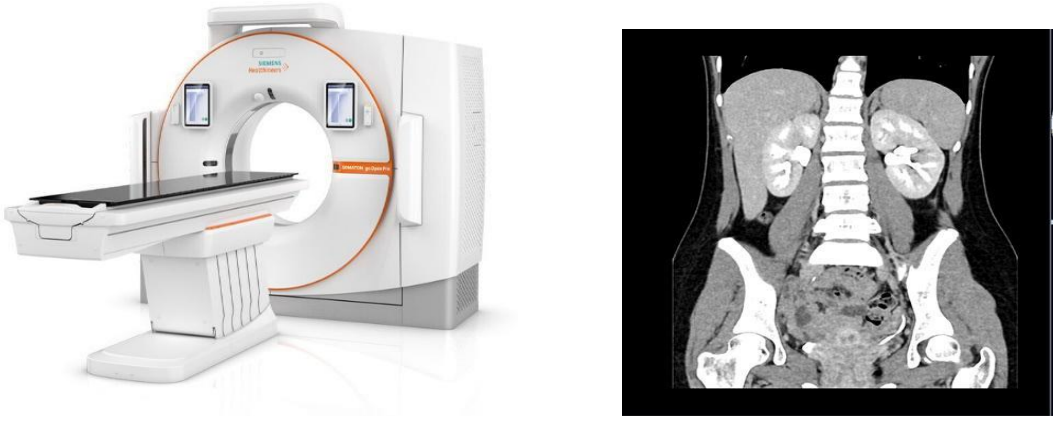

(a) (b)

**Figure 3.** Computed tomography (CT) imagery: a) CT scanner and b) CT scan for the abdomen.

### I.2.1.4. IRM images

An MRI is a computer-generated image modality, which displays images of the body in thin tomographic slices.

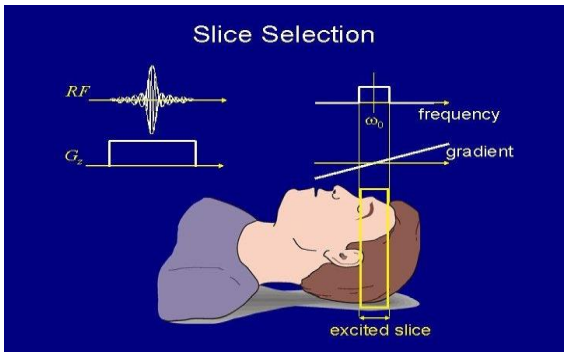


**Figure 4.** In MRI, the body is displayed in thin, tomographic slices.

Unlike CT, which requires ionizing radiation, MRI is based on safe interaction between radio waves and hydrogen nuclei in the body in the presence of a strong magnetic field. In addition to being safer than CT, MRI provides better imaging than CT. It provides better contrast between a lesion and its surrounding tissue, and it can be viewed in multiple planes of projection. In CT, one can scan either axially or semi-corneally. In magnetic resonance imaging (MRI), one can obtain images in any plane, that being the axial, sagittal, or coronal planes, or any degree of inclination.

When the body lies within a magnetic field, it becomes temporarily magnetized. This state is achieved when the hydrogen nuclei in the body align with the magnetic field. When exposed to radio waves at a specific frequency, the body sends back a radio wave signal, which is known as a "spin echo". This phenomenon (Nuclear Magnetic Resonance, "NMR") only occurs at one frequency (the "Larmor frequency") corresponding to the specific strength of the magnetic field. The spin-echo signal consists of multiple frequencies, reflecting various positions along the magnetic field gradients. When the signal is decomposed into its component frequencies (using a Fourier transform), the amplitude of the signal at each of these frequencies is proportional to the hydrogen concentration at that location, thus providing an image. Thus, spatial information in MRI is contained in the frequency of the signal, unlike X-ray-based imaging modalities such as CT [Bradley, 2000].

**Figure 5.** Magnetic resonance imaging (MRI) scanner.

.

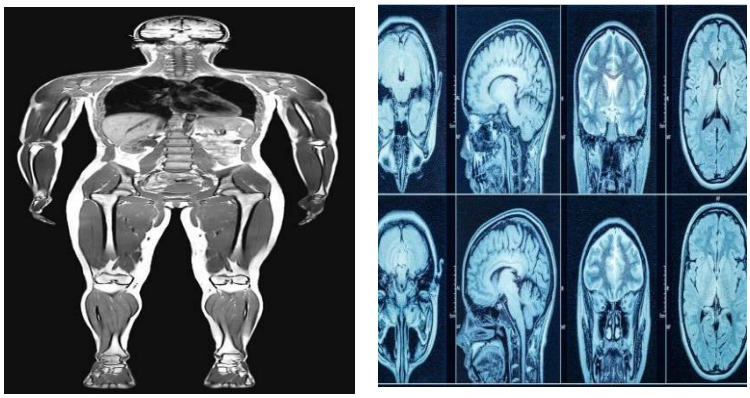

(a) (b)

**Figure 6.** Magnetic resonance imagery (MRI): a) MRI scan for the human body and b) MRI scan for the human head

### I.2.1.5. Microscopic images

An optical microscope allows for a closer view of objects that cannot be seen with normal vision. There are three main kinds of optical microscopy: light, electron, and scanning probes. Additionally, there is a new kind of microscopy called X-ray microscopy, which allows for a closer look at certain materials.

.

**Figure 7.** Microscope imagery: a) Optical microscope and b) Onion epidermis micrograph


**Figure 8.** X-ray microscope machine.

### I.2.1.6. Other data images

There are other types of biomedical image techniques, for example:

#### *Retinal*

Retinal imaging is a non-invasive diagnostic tool used to take high-definition images of the back of the eye. The technology used includes specialized cameras and scanners to magnify the retina, optic nerve, and blood vessels inside the eye [Prasad, 2022].

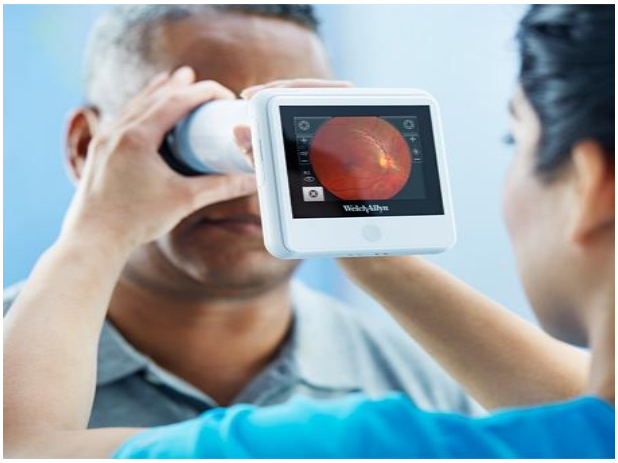

**Figure 9.** Retinal imaging.

.

#### *Ultrasound*

Ultrasound imaging (sonography) uses high-frequency sound waves to view inside the body. Because ultrasound images are captured in real-time, they can also show movement of the body's internal organs as well as blood flowing through the blood vessels [FDA, 2022].

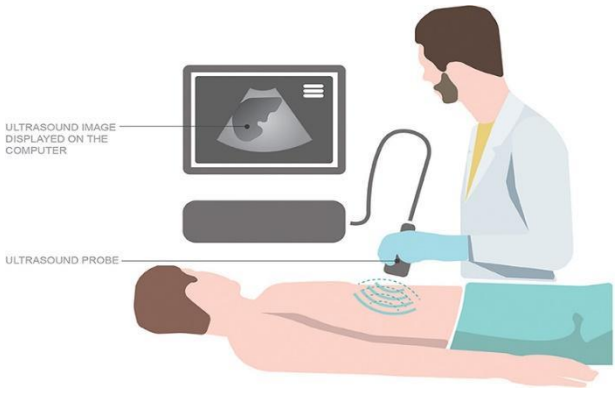


**Figure 10.** Ultrasound Imaging.

## *Endoscopy*

An endoscopy is a test to look inside your body. A long, thin tube with a small camera inside, called an endoscope, is passed into your body through a natural opening such as the mouth [NHS, 2022].

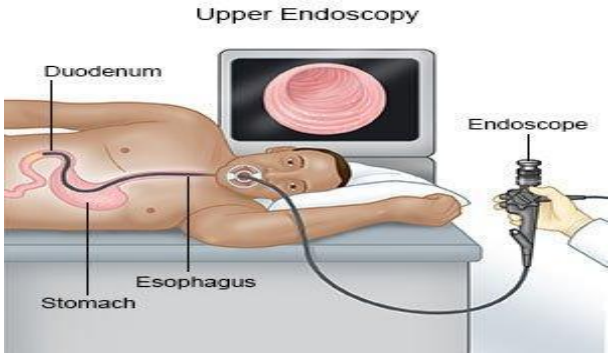


**Figure 11.** Upper endoscopy imaging.

## *Elastography*

Elastography is a non-invasive medical imaging technique that helps determine the stiffness of organs and other structures in the body. It is most commonly used to assess the liver. Elastography directs painless, low-frequency vibrations into the liver. Ultrasound (US) or magnetic resonance imaging (MRI) measures how quickly these vibrations move through the organ. A computer uses this information to create a visual map showing the stiffness (or elasticity) of the liver [RSNA, 2022].

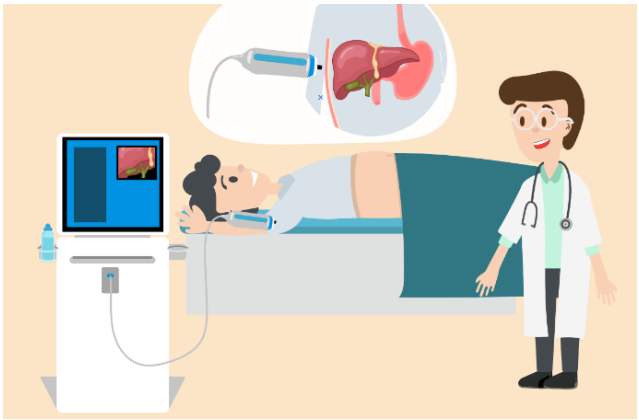

**Figure 12.** Elastography imaging.

In addition, we can cite other biomedical imaging techniques like tactile imaging, thermography, medical photography, and single-photon emission computed tomography (SPECT).

## I.3. ARTIFICIAL INTELLIGENCE

### I.3.1. Definition of AI

Artificial intelligence (AI) is a general term used to describe the use of computers to model intelligent behavior with minimal human intervention [Hamet, 2017].

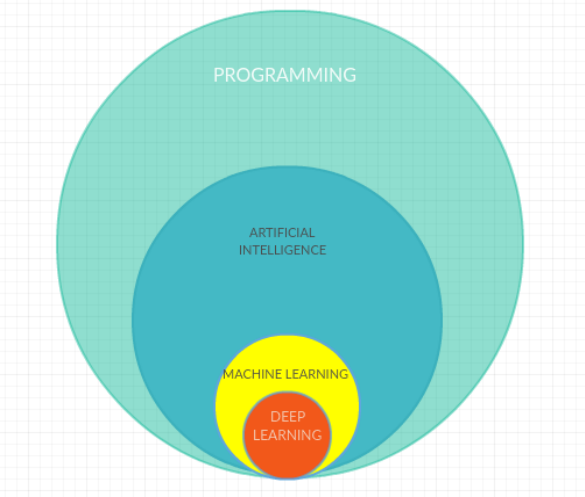


**Figure 13.** A simple definition of AI

Or like emeritus Stanford Professor John McCarthy's definition in 1955, it is the science and engineering of making intelligent machines [McCarthy, 2014]. Especially, intelligent computer programs. It is related to the similar task of using computers to understand human intelligence, but AI does not have to confine itself to biologically observable methods.

Artificial intelligence is a general term for a field that involves combining computer science and robust datasets to enable problem-solving.

Artificial intelligence includes the sub-fields of machine learning and deep learning, which are frequently mentioned together with AI.

Artificial intelligence algorithms seek to create expert systems by making predictions or classifications based on input data.

### I.3.2 Historical background

Artificial intelligence is the story that has always started with "what if" in science fiction movies. Is generally accepted as having started with the invention of robots. The word "robot"

was first coined in the 1920s by the writer Karel Capek, who used the term in his novel R.U.R. (Rossum's Universal Robots). It was a factory where bio-synthetic machines were used as forced labor. In the middle of the last century, Isaac Asimov left the word "robot" forever in his collection of modern science fiction novels. In the 12th century, a Muslim polymath, scholar, inventor, and mechanical engineer named Ismail al-Jazari created a humanoid robot that could play cymbals [Hamet, 2017].

Alan Turing was a British polymath who explored the mathematical possibility of artificial intelligence. Turing suggested that humans use available information and reasoning to solve problems and make decisions, so why can't machines do the same?

The term "AI" was coined by John McCarthy in 1955. He invented the Lisp programming language and was a key figure in organizing seminars on the Dartmouth College campus in the summer of 1956. This workshop became the starting point for modern AI research [Jaakkola, 2019].

Now, the history of artificial intelligence can be summarized as follows:

**1956** – John McCarthy coined the term 'artificial intelligence and had the first AI conference.

**1969** – Shakey was the first general-purpose mobile robot built. It is now able to do things with a purpose vs. just a list of instructions.

**1997** – The supercomputer ‘Deep Blue’ was designed, and it defeated the world champion chess player in a match. It was a massive milestone for IBM to create this large computer.

**2002** – The first commercially successful robotic vacuum cleaner was created.

**2005** – **2019** – **Today**, we have speech recognition, robotic process automation (RPA), a dancing robot, smart homes, and other innovations making their debut.

**2020** – Baidu releases the Linear Fold AI algorithm to medical and scientific medical teams developing a vaccine during the early stages of the SARS-CoV-2 (COVID-19) pandemic. The algorithm can predict the RNA sequence of the virus in only 27 seconds, which is 120 times faster than other methods.

### I.3.3. History of artificial intelligence in medicine:

Artificial Intelligence in Medicine (AIM) has evolved significantly over the past five decades. Applications of AI have expanded since the advent of machine learning and deep learning, creating opportunities for personalized healthcare rather than algorithm-only

medicine. Predictive models can help diagnose diseases, predict therapeutic responses and potentially provide preventive medicine in the future [Kaul, 2020].

The figure below represents a brief historical perspective of the advent of AI in medicine and its chronological evolution through the last half-century:

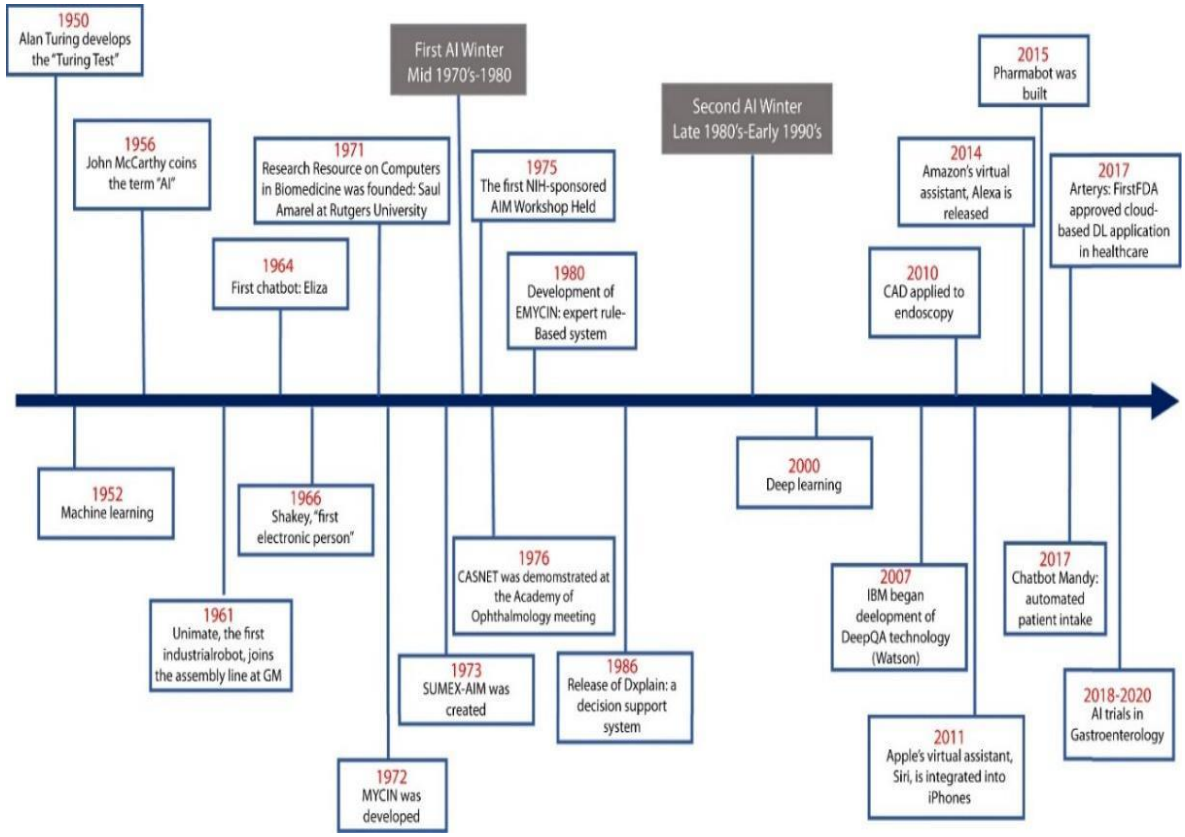


**Figure 14.** Timeline of the development and use of artificial intelligence in medicine [Kaul, 2020].

### I.3.4. AI algorithms

AI systems are based on large, intelligent processing algorithms that are constantly evolving. This algorithm allows AI to learn from patterns and features in the data. Each time an AI system processes data, it tests its performance and uses the results to improve its abilities.

### I.3.5. Machine learning techniques

Machine learning is a set of algorithms that can be used to complete tasks without being specifically programmed.

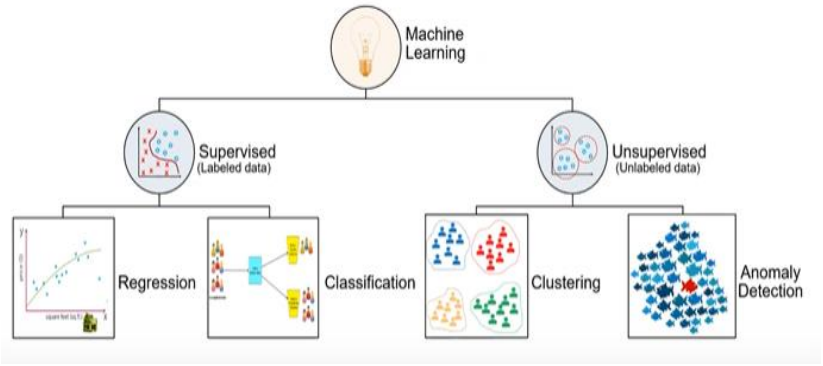


**Figure 15.** Overview of machine learning techniques.

There are many different types of machine learning algorithms, which can be broken down like this into this table:

**Table 1.** Machine learning algorithms.

| **Algorithm** | **Type of the task** |
|---|---|
| Artificial Neural networks | Classification/Regression |
| Support Vector Machine | Classification |
| Naive Bayes | Classification |
| Random forest | Classification/Regression |
| Linear regression | Classification/Regression |
| K-means | Clustering |
| Canonical correlation analysis | Feature extraction |
| Principal component analysis | Feature extraction and dimensionality reduction |
| K-nearest neighbor | Classification |

In the following points, we will discuss only the three well-known machine learning techniques, such as K-nearest neighbors, support vector machines, and artificial neural networks.

### I.3.5.1. KNN (K-nearest neighbors)

K-Nearest Neighbors (KNN) is a classification algorithm that classifies a new unseen data point by looking for the K nearest neighbors in the training set that is closest to it in the feature space.

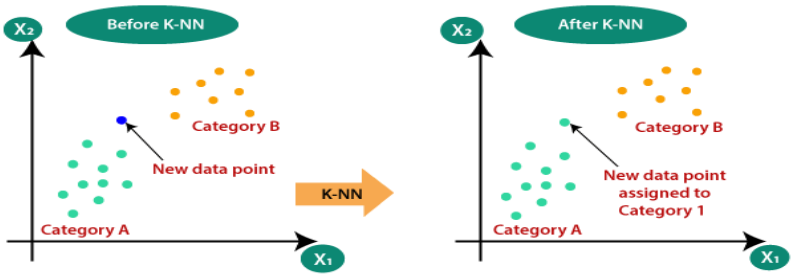


**Figure 16.** K-nearest neighbors (KNN).

### I.3.5.2. SVM (Support Vector Machines)

A support vector machine (SVM) learns by example to assign labels to objects.

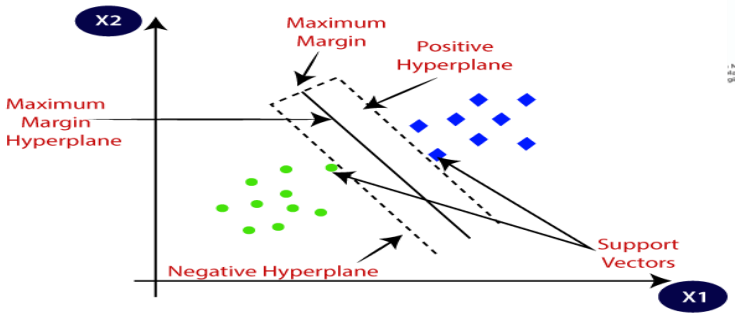


**Figure 17.** Support Vector Machines (SVM).

### I.3.5.3. Artificial Neural Networks (ANNs)

Artificial neural networks (ANNs) are a subfield of machine learning, in which the Research into ANNs started after McCulloch and Pitts (1943) proposed a mathematical model of neuronal activity in the brain. The goal behind ANNs was to develop machine learning systems that imitates a biological function of the brain, specifically, the bioelectrical activity of the neurons in the brain [Walczak, 2018]. Therefore, ANNs are comparatively basic electronic models inspired by the brain's neural structure [Anderson, 1992]. They have neurons that are

interconnected to one another in various layers of the networks. These neurons are known as nodes.

Natural neurons receive signals through synapses located on the Dendrites of the neuron. Once the signals received are strong enough (surpass a certain threshold), the neuron is activated and emits a signal through the Axon. This signal may well be sent to a different synapse, and would possibly activate other neurons [Gershenson, 2003].

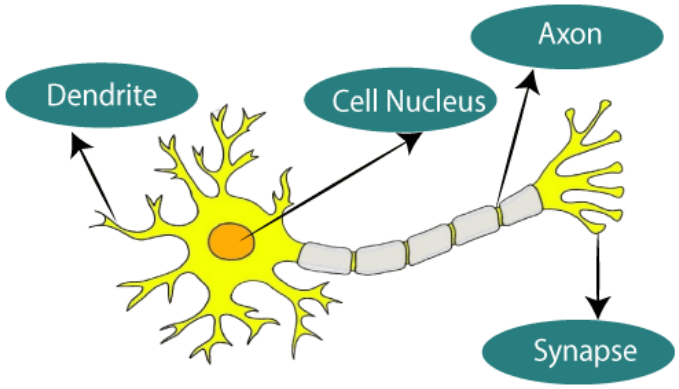


**Figure 18.** Typical diagram of Biological Neural Network.

Artificial neurons consist of inputs (like synapses) that are multiplied by weights (strengths of the respective signals), and then calculated by a mathematical function that determines the activation of the neuron. Another function (which can be the identity) computes the output of the artificial neuron (sometimes based on a certain threshold). ANNs combine artificial neurons to process information [Gershenson, 2003].

We could say that artificial neurons simulate the four basic functions of natural neurons. Figure II.7 shows a fundamental representation of an artificial neuron.

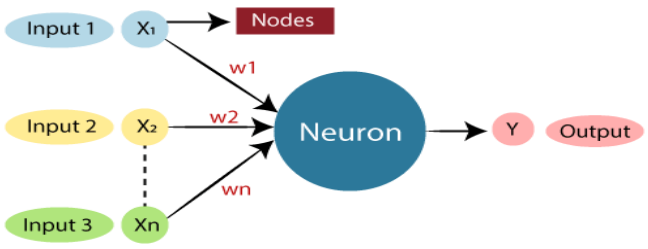


**Figure 19.** Artificial neural network (ANN).

Table 2 demonstrates relationship between biological neural networks and artificial neural networks:

**Table 2.** Relationship between Biological neural network and artificial neural network.

| Biological Neural Network | Artificial Neural Network |
|---|---|
| Dendrites | Inputs |
| Cell nucleus | Nodes |
| Synapse | Weights |
| Axon | Output |

## I.4. Deep learning

Deep learning is a branch of machine learning that learns to represent the world as a nested hierarchy of concepts and representations, with each concept explained in terms of simpler ones and more abstract representations computed in terms of less abstract ones [Bengio, 2017].

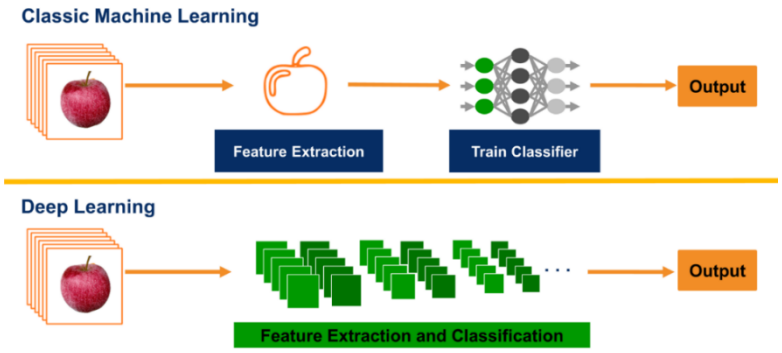


**Figure 20.** The difference between Machine learning and deep learning.

Two main ideas drive the neural perspective on deep learning. One concept is that the brain empowers as proof that intelligent behavior is possible and that reversing engineering the brain's computational principles and replicating its functionality is a conceptually simple path to building intelligence. Apart from their ability to solve engineering problems, learning models that shed light on these fundamental scientific questions are useful [Goodfellow, 2016].

Deep learning allows computational models with multiple processing layers to learn multiple levels of abstraction for data representations. These techniques have vastly improved

the state-of-the-art in object detection, speech recognition, visual object recognition, and a variety of other fields like drug discovery and genomics. Deep learning uses the backpropagation algorithm to show how a machine should change its internal parameters that are used to compute the representation in each layer from the representation in the previous layer, revealing intricate structures in large data sets. Deep convolutional networks have revolutionized image, video, speech, and audio processing, while recurrent nets have shed light on sequential data like text and speech [LeCun, 2015].

### I.4.1. Deep learning techniques

Deep learning techniques surpasses the machine learning ones, and they have grown in popularity as the amount of data available increased, as did the advancement of hardware that provides powerful computers. DL algorithms process data in layers; each layer extracts features progressively and passes them on to the next layer. The first layers extract low-level features, and the subsequent layers combine them to form a complete representation [Mathew, 2020]. Figure 21 represents the process (layers) behind the classification of a medical image.

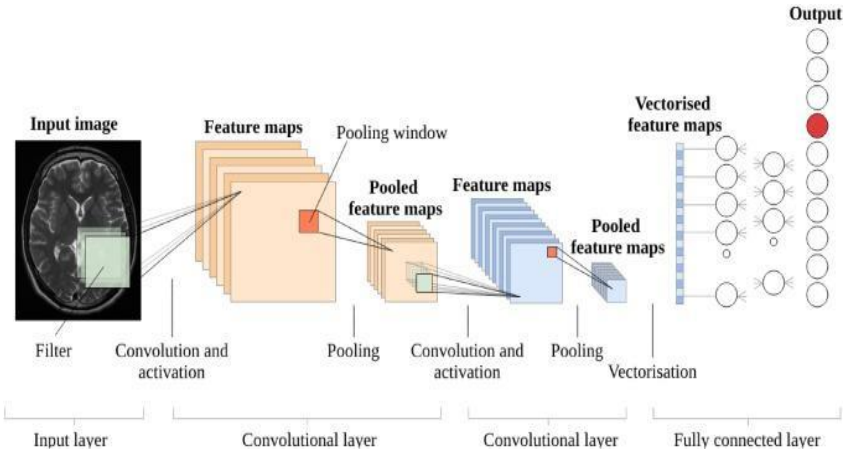


**Figure 21.** Overview of deep learning in medical imaging.

We have seen numerous DL techniques up to this point, each with a unique feature that distinguishes it from the others. As a result, in the following points, we will just take some of them and describe the meaning behind them, with a focus on Convolutional Neural Networks (CNN) because we will be working with them.

#### I.4.1.1. Long Short-Term Memory (LSTM)

(LSTM) A popular type of RNN architecture that utilizes special units to solve the vanishing gradient problem [Hochreiter, 1997].

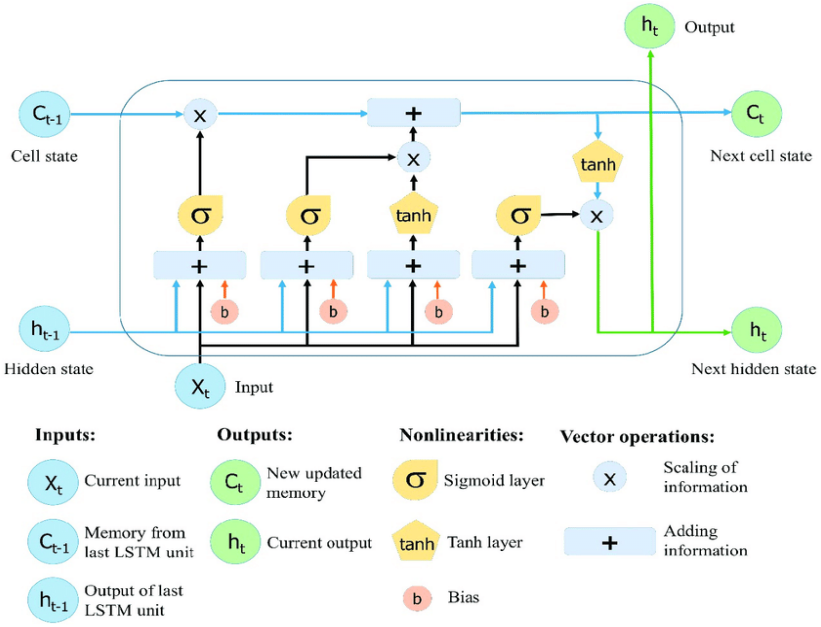


**Figure 22.** The structure of the Long Short-Term Memory (LSTM) neural network.

### I.4.1.2. Deep Boltzmann Machine (DBM)

Deep Boltzmann machines are undirected networks of interconnected units that tweak connections between them to learn a joint probability density over these units. In theory, they can learn statistically and computationally efficient representations of apparently complex data distributions. Developing an algorithm that properly learns the data representation can be tough. The parameterization of the energy function of deep Boltzmann machines is sensitive. Furthermore, the gradient of the optimization issue is not readily accessible and must instead be approximated stochastically by querying the model continuously throughout training [Montavon, 2012].

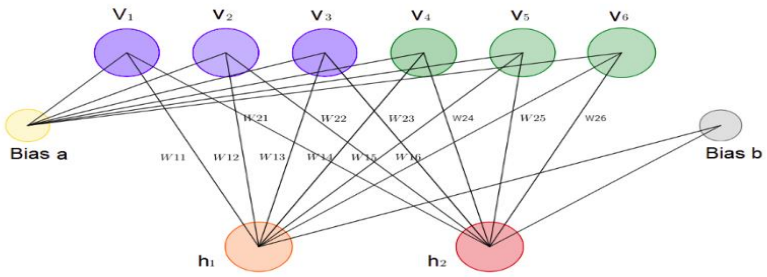


**Figure 23.** A Deep Boltzmann Machine diagram.

### I.4.1.3. Auto Encoder

An auto-encoder (AE) is a well-known unsupervised learning technique that employs neural networks to learn representations. Auto-encoders are implemented to operate with high-dimensional data, and dimensionality reduction specifies how a data set is represented. An autoencoder is made up of three parts: an encoder, a code, and a decoder. The encoder compresses the input and generates the code, which is then used by the decoder to reconstruct the input. Recently, AEs have been utilized to learn generative data models. Many unsupervised learning applications, including dimensionality reduction, feature extraction, efficient coding, generative modeling, denoising, anomaly or outlier detection, and so on, make extensive use of the auto-encoder [Sarker, 2021].

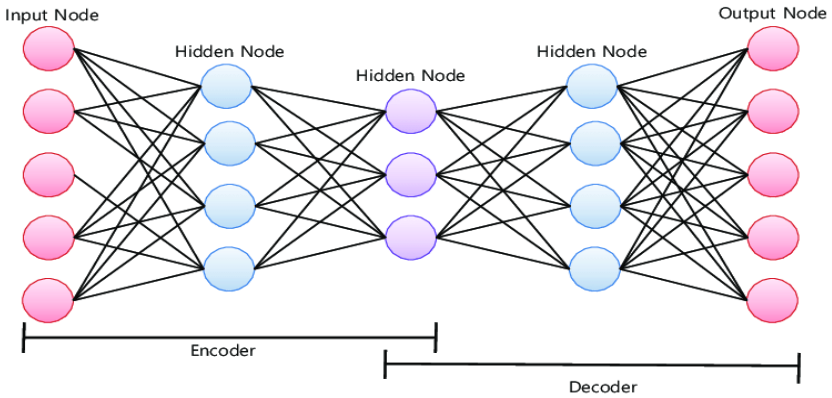


**Figure 24.** Structure of auto-encoder [Nam, 2018].

### I.4.1.4. CONVOLUTIONAL NEURAL NETWORKS (CNNs)

#### Principle

The term "convolutional neural network" refers to the network's use of the mathematical operation convolution, which is a subset of linear operations. Convolutional networks are simple neural networks with at least one layer that uses convolution instead of ordinary matrix multiplication [Goodfellow, 2016].

Convolutional neural networks (CNNs) are mostly utilized for image processing. It assigns weights and biases to various objects in the image and separates them [Mathew, 2020].

Natural images contain various statistical features that are not affected by translation. An image of a cat, for example, remains an image of a cat if it is translated one pixel to the right. CNN takes this fact into consideration by sharing parameters across several image locations. The same feature (a hidden unit with the same weights) is computed over different locations in the input. This demonstrates that we can use the same cat detector to discover a cat in the image whether it appears in column I or column I + 1 [Goodfellow, 2016].

#### Historical background

In 1990, LeCun and his colleagues [LeCun, 1995] published a seminar paper that established the modern framework of CNN. Later, they enhanced it in [LeCun, 1998], by which they developed LeNet-5, a multi-layer artificial neural network that can classify handwritten digits. LeNet-5, like all other neural networks, contains numerous layers and is trainable using the backpropagation algorithm [Hecht-Nielsen, 1992]. It is capable of obtaining excellent representations of the original image, allowing it to recognize visual patterns directly from raw pixels with little to no preprocessing [Gu, 2018].

#### CNN architecture

Convolutional neural networks are made up of three different types of layers. Convolutional layers, pooling layers, and fully-connected layers.

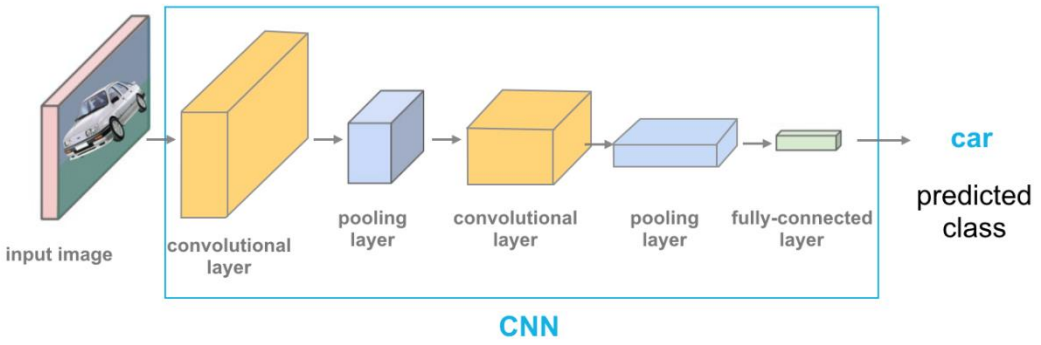


**Figure 25.** Typical CNN Architecture.

## Convolution layer

CNNs are so-named because of the convolutional layers in their architecture [Tajbakhsh, 2016]. Convolutional layers are generated from a series of filters (also referred to as kernels) that are applied to an input image. The convolutional layer creates a feature map, which is a representation of the input image after the filters have been applied. Convolutional layers can be stacked to create more sophisticated models that can learn more intricate features from images [Kumar, 2022].

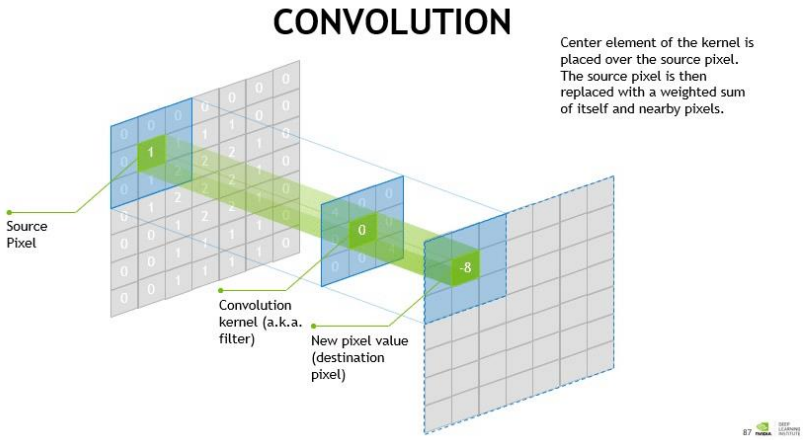


**Figure 26.** The convolutional operation (Nvidia).

## Pooling layer

A pooling layer is often placed between two convolutional layers. By down-sampling the representation, the pooling layer minimizes the number of parameters and processing. The pooling function might be either max or average. Max pooling is often used because it works better [Ke, 2018].

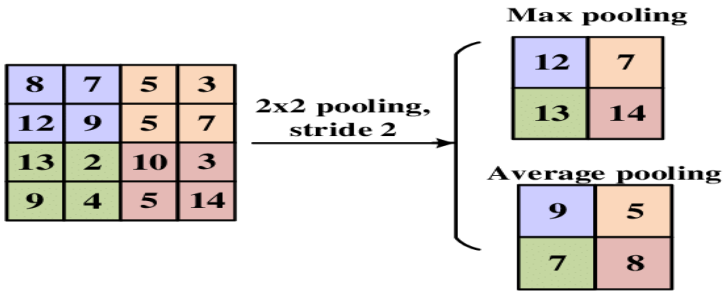


**Figure 27.** Max pooling & average pooling [Yingge, 2020].

## Rectified Linear Unit (ReLU)

ReLU is utilized as an activation function in the model to improve nonlinearity and performance. Each convolutional block gets the ReLU activation layer. This layer significantly reduces the linearity of the extracted features. Furthermore, it increases the model's ability to predict a more diverse set of input data. ReLU can also incorporate more nonlinearity into the model [Kim, 2021]. So, all negative feature values are replaced with zeros.

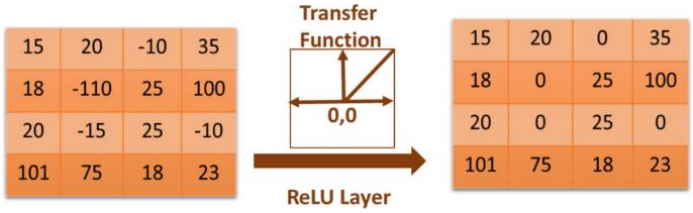


**Figure 28.** Process of ReLU as a transfer function [Kim, 2021].

## Fully connected layer

The fully connected layer is typically utilized for classification at the end of the network. It receives input from feature extraction stages and analyses the output of all previous layers globally. As a result, it creates a non-linear combination of selected features for data classification [Khan, 2020].

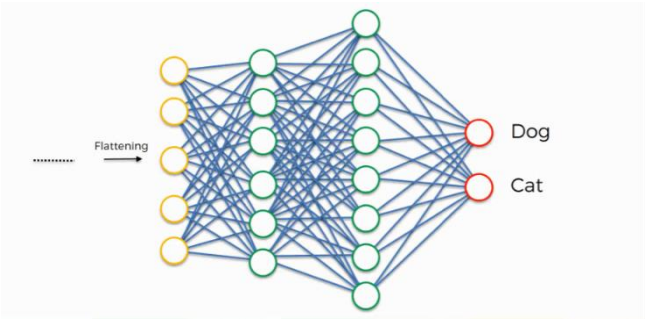

**Figure 29.** The fully connected layer in neural network

## Softmax

Softmax is a mathematical function that transforms a vector of numbers into a vector of probabilities, with the probability of each value begin proportional to the vector's relative scale. The softmax function is most commonly used in applied machine learning as an activation function in a neural network model. The network is specifically set to produce N values, one for each class in the classification task, and the softmax function is used to normalize the outputs, transforming weighted sum values into probabilities that total to one. Each value in the softmax function output is regarded as the likelihood of membership in each class [Brownlee, 2022].

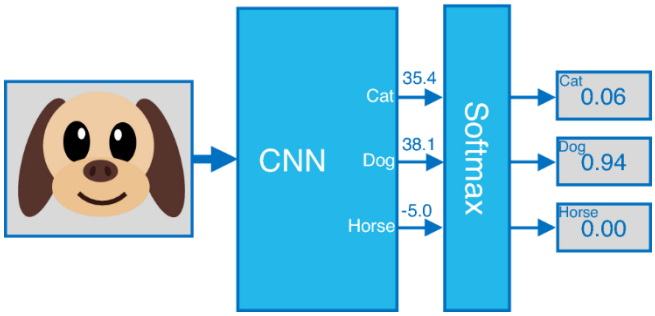


**Figure 30.** Softmax function [Cardarilli, 2021].

## Dropout

The dropout technique can be used to solve the overfitting problem in deep neural networks. During training, this strategy is used by randomly eliminating units and their connections. Dropout is a powerful regularization approach to reduce overfitting and improve generalization error. Dropout improves supervised learning performance in computer vision, computational biology, document categorization, and speech recognition [Mathew, 2020].

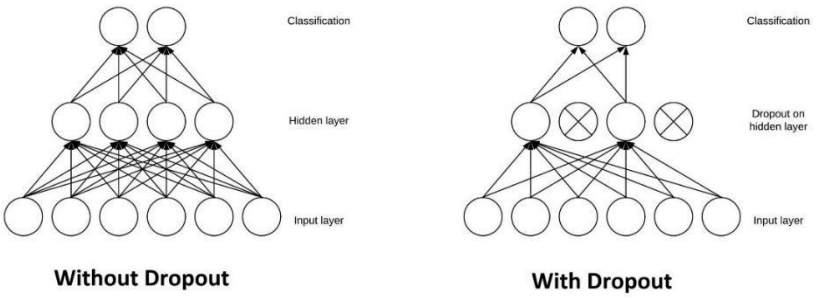


Figure 31. Overview of how dropout works in the hidden layers (building).

### I.4.1.2. CNN model types

#### I.4.1.2.1. LeNet

The first CNN architecture is LeNet. Yann LeCun, Corinna Cortes, and Christopher Burges created it in 1998 to solve handwritten digit recognition problems. It is one of the first and most extensively used CNN architectures, The LeNet architecture is made up of many convolutional and pooling layers, which are followed by a fully-connected layer. Five convolution layers are followed by two fully connected layers in the model. However, due to the vanishing gradient problem, LeNet was unable to train effectively. To overcome this limitation, a shortcut connection layer known as max-pooling is employed between convolutional layers to reduce image spatial size, hence preventing overfitting and allowing CNNs to train more successfully [Kumar, 2022].

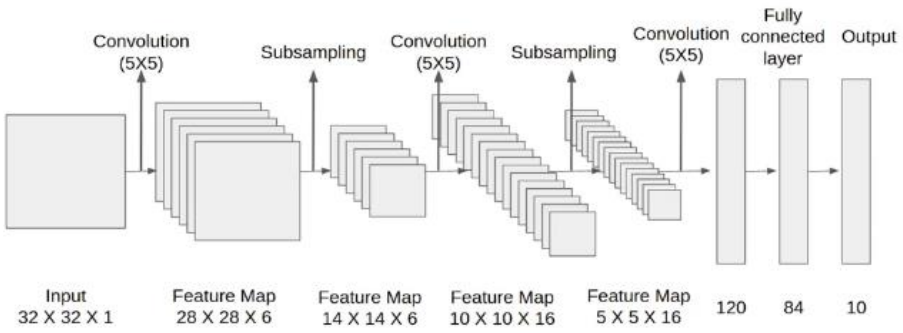


**Figure 32.** LeNet5 architecture.

#### I.4.1.2.2. ImageNet

ImageNet is a dataset of over 15 million labeled high-resolution images belonging to roughly 22,000 categories. The architecture contains eight learned layers, five convolutional and three fully connected [Krizhevsky, 2012].

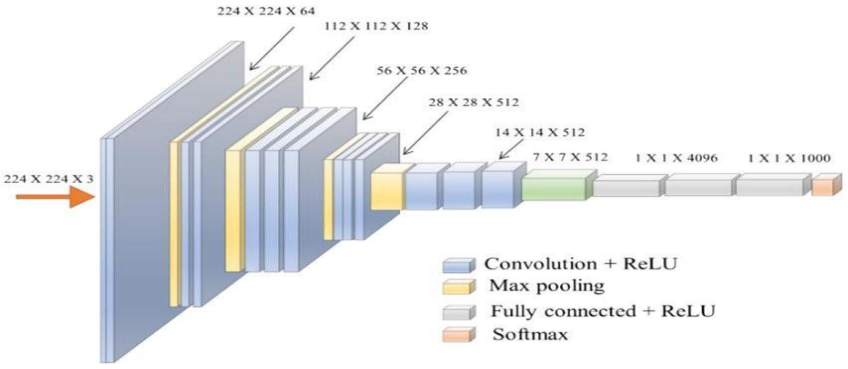


**Figure 33.** ImageNet architecture.

### I.4.1.2.3. VGG-Net

VGG stands for Visual Geometry Group, and VGG-Net is the CNN architecture developed at Oxford University by Karen Simonyan, Andrew Zisserman, et al [Simonyan, 2014]. There are six VGGNet Architectures in total (VGG-11, VGG-11(LRN), VGG-13, VGG-16(Conv1), VGG-16 and VGG-19). VGG-16 and VGG-19 are two of the most well-known. The precise structure of the VGG-16 network is presented in Figure I.34:

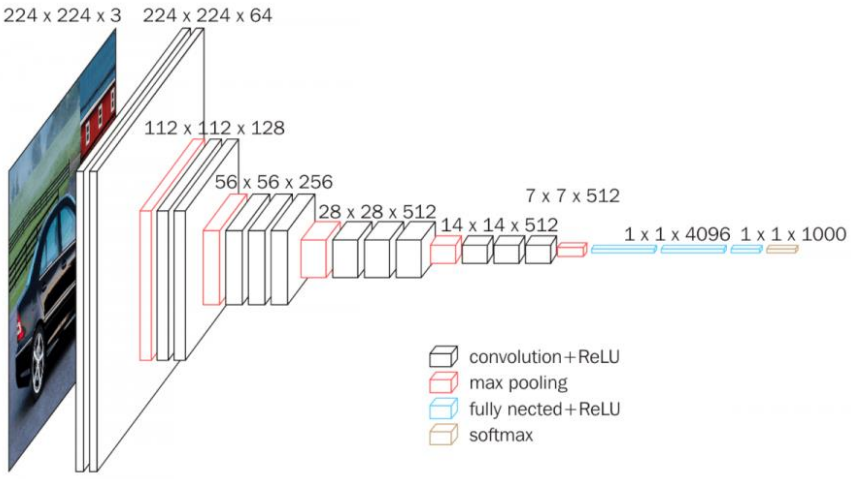


**Figure 34.** VGG-Net architecture.

.

VGG-16 has a total of 16 layers, with 13 convolutional and 3 fully connected layers [Kim, 2021].

VGG takes an RGB image with a resolution of 224x244 pixels as its input. The average RGB value for all images on the training set image is determined, and the image is then sent into the

VGG convolution netwl2ork as an input. The convolution step is fixed and a 3x3 or 1x1 filter is utilized. There are 3 VGG fully connected layers, with the total number of convolutional layers + fully connected layers varying from VGG11 to VGG19. VGG11 contains a minimum of 8 convolutional layers and 3 fully connected layers. VGG19 has a maximum of 16 convolutional layers where +3 layers that are fully connected [Varshney, 2020].


**Figure 35.** VGG Network layers.

The most noticeable enhancement to VGG-Net is the reduction in the size of the convolution kernel while increasing the number of convolution layers. Using multiple convolution layers with smaller convolution kernels instead of a larger convolution layer with convolution kernels can reduce parameters on the one hand, and the author believes that it is equivalent to more non-linear mapping, which increases the Fit expression ability [Varshney, 2020].

### I.4.1.2.4. MobileNet

MobileNet is a type of convolutional neural network designed for mobile and embedded vision applications. They are based on a streamlined architecture that uses depthwise separable convolutions to build light weight deep neural networks that can have low latency for mobile and embedded devices [Howard, 2017].

The MobileNet model is based on depthwise separable convolutions, a form of factorized convolution that factors a standard convolution into a depthwise convolution and a pointwise convolution. Depthwise convolution in MobileNets applies a single filter to each input channel. The depthwise convolution outputs are then combined using a 1 x 1 convolution by the pointwise convolution. In a single step, a standard convolution filters and combines inputs to produce a new set of outputs. The depthwise separable convolution splits this into two layers,

one for filtering and one for combining. This factorization results in significant reductions in computation and model size [Howard, 2017].

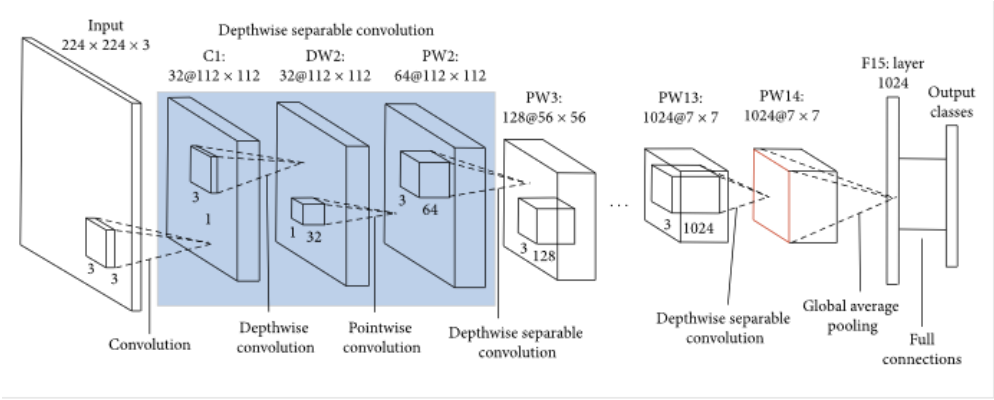


**Figure 36.** MobileNet architecture.

***MobileNet V2***

According to [Sandler, 2018], MobileNet V2 enhances mobile model performance on multiple tasks and benchmarks, as well as across a spectrum of model sizes.

In MobileNet V2, each block contains a 1 x 1 expansion layer in addition to a depthwise and a pointwise convolutional layer. Unlike V1, the pointwise convolutional layer of V2 known as the projection layer projects data with a high number of channels into a tensor with a much lower number of channels. The bottleneck residual block has the output of each block is a bottleneck. A 1 x 1 expansion convolutional layer will expand the number of channels depending on the expansion factor in the data before it goes into the depthwise convolution. The second new thing in MobileNet V2's building block is the residual connection. The residual connection exists to help the flow of gradients through the network. Each layer of MobileNet V2 has batch normalization and the ReLU6 as the activation function. However, the output of the projection layer does not have an activation function. The full MobileNet V2 architecture consists of 17 bottleneck residual blocks in a row followed by a regular 1×1 convolution, a global average pooling layer, and a classification layer [Michele, 2019].

### I.4.2. CNN Training Modes

#### I.4.2.1. Transfer learning

Transfer learning research is driven by the idea that humans can intelligently apply previously learned knowledge to solve new problems faster or with better solutions. The primary motivation for transfer learning in machine learning was explored in a Neural

Information Processing Systems (NIPS-95) workshop on "Learning to Learn," which emphasized the need for lifelong machine learning approaches that preserve and utilize previously learned knowledge [Pan, 2009].

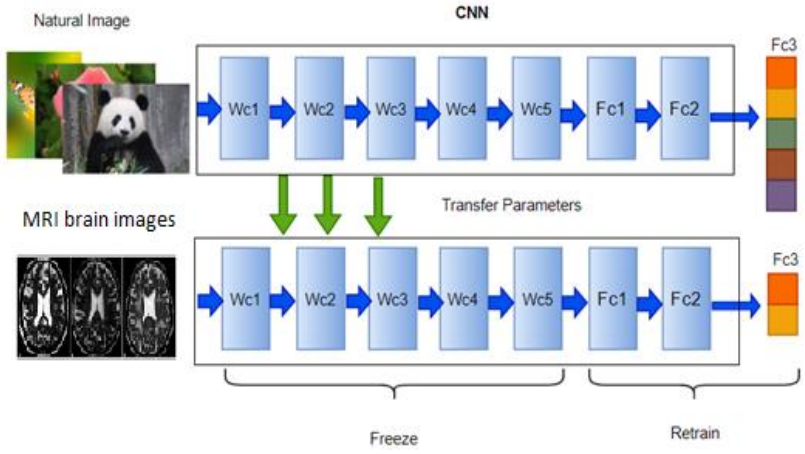


**Figure 37.** The process of transfer learning technique.

Transfer learning requires initially training a base network on a base dataset and task, and then repurposing or transferring the learned features to a second target network to be trained on a target dataset and task. This process is more likely to succeed if the features are general, that is, applicable to both the base and target tasks, rather than specific to the base task [Yosinski, 2014].

### I.4.2.2. Fine-tuning

Fine-tuning is a popular transfer learning technique for deep neural networks where a few rounds of training are applied to the parameters of a pre-trained model to adapt them to a new task. In the standard fine-tuning, we either optimize all the pretrained parameters or freeze certain layers (often the initial layers) of the pre-trained model and optimize the rest of the layers toward the target task [Guo, 2020].

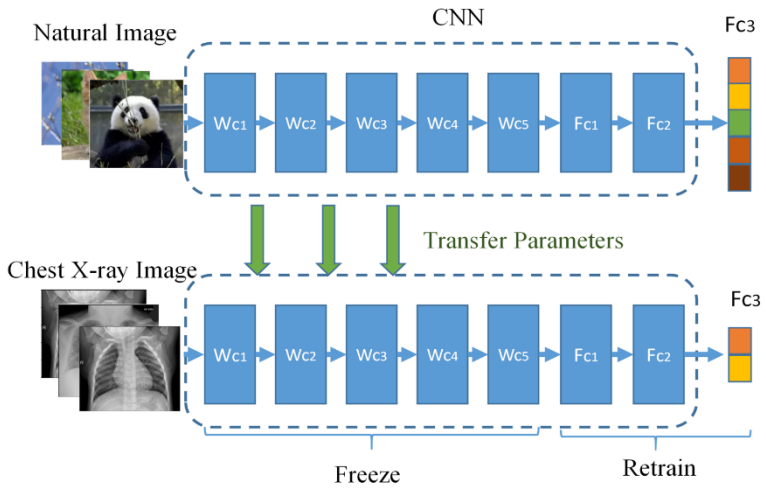


**Figure 38.** The process of Fine-tuning technique.

## CONCLUSION

In this chapter, we covered biological data and how broad this sector is, as well as what artificial intelligence is and what it encompasses.

In the second chapter, we will see the method proposed and we will go into more detail about Alzheimer's disease image classification using CNN.

# Chapter II: Proposed Alzheimer's disease diagnosis system

## INTRODUCTION

In this chapter, we discuss the state of the art of Alzheimer's diagnosis in the last years. Then, we propose our Alzheimer's disease diagnosis system and its components. A detailed description of each part of our system is provided to give an idea about the methods and techniques used in this work.

## II.1. ALZHEIMER DISEASE

The most common cause of dementia is Alzheimer's disease (AD) because 60–80% of dementia cases account for it. In a neurodegenerative form of dementia, AD is a chronic, irreversible brain disorder. There has been no effective cure for it till now. AD starts with cognitive impairment (CI) and gradually gets worse. It affects brain cells, induces memory loss, and thinking skills, and hinders the performance of simple tasks. Therefore, AD is a progressive, multi-faceted neurological brain disease. People with CI are more likely to develop AD than others. People observe the effects of AD only after years of changes in the brain because it takes two decades or more before the symptoms are detected. Alzheimer's Disease International (ADI) reports that more than 50 million people worldwide are dealing with dementia. By 2050, this percentage is projected to increase to 152 million people, which means that every 3 seconds; someone develops dementia [Helaly, 2021].

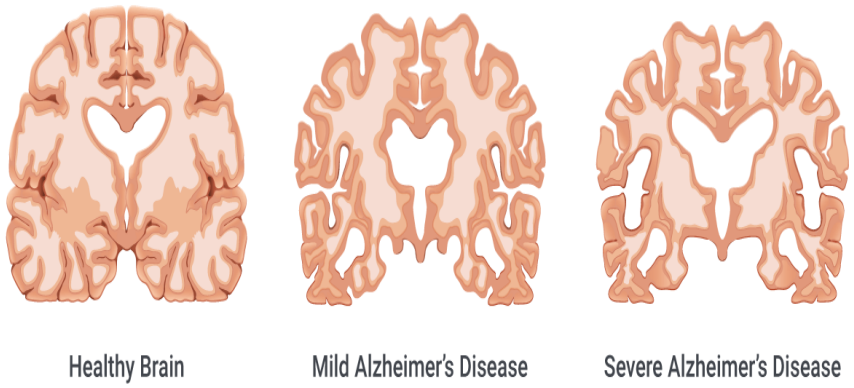


**Figure 39.** Progression of Alzheimer's disease.

The biggest challenge facing Alzheimer's experts is that there is no reliable treatment available for an AD so far. Despite this, current AD therapies can relieve or slow down the progression of symptoms. So, the early detection of AD at its prodromal stage is critical. A Computer-Aided System (CAD) is used for accurate and early AD detection to avoid AD patients' high care costs, which are expected to rise dramatically. In early AD diagnosis, traditional machine learning techniques typically take advantage of two types of features: region of interest (ROI)-based features and voxel-based features. More specifically, they rely heavily on basic assumptions, such as regional cortical thickness, hippocampal volume, and gray matter volume, regarding structural or functional anomalies in the brain [Helaly, 2021].

Traditional methods depend on manual feature extraction, which relies heavily on technical experience and repetitive attempts, which appear to be time-consuming and subjective. As a result, deep learning, especially with convolutional neural networks (CNNs), is an effective way to overcome these problems. CNN can boost efficiency further, has shown great success in AD diagnosis, and it does not need to do handcrafted feature extraction as it extracts the features automatically [Helaly, 2021].

## II.2. ALZHEIMER'S DIAGNOSIS STATE OF THE ART

Alzheimer's disease is one of the most common forms of dementia. With no valid cure or precise clinical diagnosis to it. By using deep learning techniques, we probably could make an early diagnosis model that can prevent the development of the disease. The majority of early Alzheimer's disease detection approaches were based on the classification of characteristics taken from brain scans, with features claimed to accurately represent AD-related alterations of physical brain structures. These features are typically supplied into deep learning algorithms for classification.

Many researchers have relied on artificial intelligence for the early detection of this disease by applying different techniques. We will see the most important studies and results of the past few years.

Kundaram and his colleagues [Kundaram et al, 2021] presented their model using the deep CNN technique (DCNN). The architecture consists of three sets of convolutional and max-pooling layers, followed by a flattening convolutional layer feature, two fully connected layers, and finally a SoftMax/sigmoid classifier. Output has three classes, which are Alzheimer's

disease (AD), normal control (NC), and mild cognitive impairment (MCI). The input for architecture is a 256 × 256 grayscale image, which passes through the first convolutional layer with 32 feature maps with filters having a size 3 × 3, a stride of one, and pooling is made zero with the ReLU activation function. They have achieved 98.57% accuracy on their dataset without using any handcrafted features for training the network. The validation accuracy achieved is 87.72%. Experimental data are obtained from ADNI, and a total of 13,733 images from 266 subjects are used.

In [Budhiraja et al., 2021], they present transfer learning-based Alzheimer's disease classification models from MRI images. In which they tested five popular models, namely CNN, DenseNet 169, ResNet 50, VGG 19, and Inception V3, they used the pre-trained weights of ImageNet in the base model and fine-tuned our model on the dataset to get more accurate results.

Hon et al. [Hon et al., 2017] propose a transfer learning-based method to detect AD from structural MRI images. They tested two popular architectures, namely VGG16 and Inception V4. Through pre-trained weights from ImageNet and fine-tuning, they can only use a small number of training images to obtain highly accurate results. Moreover, they employ an intelligent entropy-based technique to select the training dataset in a way that represents the maximum amount of information within a small set. They tested their models on images from the OASIS brain imaging dataset, where 6,400 images extracted from MRI scans of 200 subjects were used to train the models. The target was to differentiate AD patients from healthy control (HC) by analyzing MRI scan data through the CNN architecture. by using structural MRI data from the Open Access Series of Imaging Studies (OASIS). OASIS provides two types of data: cross-sectional and longitudinal. Their target was to simply differentiate between AD and HC patients through the images, so they used cross-sectional data. The dataset consists of 416 subjects whose ages are between 18 and 96. In the experiments, they randomly picked 200 subjects, 100 of whom were picked from the AD group, and the other 100 from the HC group. The grouping was determined by the Clinical Dementia Rating (CRD) variable, ranging from 0 to 2. The assumption is that a 0 implies HC and those greater than 0 are AD. Which is like if CDR (Clinical Dementia Rating): 0 = nondemented, 0.5 = very mild dementia, 1 = mild dementia, 2 = moderate dementia, CDR > 0: probable AD. To test the generalization power of transfer learning, they only used a limited number of images from these scans to train the networks. They used their entropy-based sorting mechanism to pick the most informative 32 images from the axial plane of each 3D scan. That resulted in a total of 6400 training images,

3200 of which were AD and the other 3200 were HC. To be compatible with the pre-trained models of VGG16 and Inception V4, the images were resized to be 150x150 for VGG16 and 299x299 for Inception V4 [Hon, 2017].

Cui and his colleagues [Cui et al., 2018] have proposed a new classification framework based on a combination of CNN and bidirectional gated recurrent units (BGRU) for the longitudinal analysis of time series structural MR images for AD diagnosis. The Multi-Layer Perceptron (MLP) model extracts the spatial features and generates a single-time classification result, while BGRU extracts the temporal features for the longitudinal classification. This method can automatically learn the spatial and longitudinal features from the imaging data of multiple time points with the variable-length for classification. The method is evaluated using T1-weighted structural MR images of 428 subjects, including 198 AD patients and 229 normal controls (NC) from the Alzheimer's Disease Neuroimaging Initiative (ADNI) database. Experimental results show the proposed method achieves an accuracy of 89.7% for AD classification.

The proposed system by [Maqsood et al, 2019] works on an efficient technique of utilizing transfer learning to classify the images by fine-tuning a pre-trained convolutional network, AlexNet. The architecture is trained and tested over the pre-processed segmented (Grey Matter, White Matter, and Cerebral Spinal Fluid) and un-segmented images for both binary and multi-class classification. The performance of the proposed system is evaluated over the Open Access Series of Imaging Studies (OASIS) dataset. The algorithm showed promising results by giving the best overall accuracy of 92.85% for multi-class classification of un-segmented images.

Also, Ghazal and his colleagues [Ghazal et al., 2022] proposed a system for Alzheimer's disease detection utilizing transfer learning on multi-class classification using brain magnetic resonance imaging (MRI) to classify the images into four stages: mild demented (MD), moderate demented (MOD), non-demented (ND), and very mild demented (VMD). Simulation results have shown that the proposed system model gives 91.70% accuracy.

We summarize all of the above in the following Table 3.

**Table 3.** State of the art.

| Reference | Dataset | Dataset size (image) | | class | Method | model | validation accuracy (%) |
|---|---|---|---|---|---|---|---|
| | | training data | testing data | | | | |
| [Kundaram, 2021] | ADNI | 9540 | 4193 | 3 | DCNN | Designated model | 87.72 |
| [Budhiraja, 2021] | ADNI from Kaggle | 3842 | 1279 | 4 | CNN | VGG-19 | 76.90 |
| | | | | | CNN | Inception-V3 | 78.70 |
| | | | | | CNN | Resnet-50 | 79.20 |
| | | | | | CNN | CNN | 75.60 |
| | | | | | CNN | DensNet-169 | 82.50 |
| [Hon, 2017] | OASIS | 5120 | 1280 | 2 | CNN | VGG16(from scratch) | 74.12 |
| | | | | | CNN | VGG16 (transfer learning) | 92.3 |
| | | | | | CNN | InceptionV4 (transfer learning) | 96.25 |
| [Cui, 2018] | ADNI | _ | _ | 5 | CNN+RNN | MLP+BGRU | 89.69 |
| [Maqsood, 2019] | OASIS | 382 | | 4 | CNN | AlexNet | 92.85 |
| [Ghazal, 2022] | Kaggle repository | 5115 | 1278 | 4 | CNN | ADDTLA | 91.70 |

## II.3. PROPOSED ALZHEIMER DIAGNOSIS SYSTEM

According to our research, it is rare to achieve accuracy levels above 99 percent, which is a problem if we want to implement our approaches in hospitals or clinics. As a result, we propose a system with high accuracy and stability to detect Alzheimer's in three classes: AD (Alzheimer's Disease), CI (Cognitive Impairment), and CN (Cognitively Normal). To make the decision, the system uses deep learning algorithms to process and learn patterns. CNNs were

chosen to assist us in this quest. We trained our system on two different models (VGG16 & MobileNetV2).

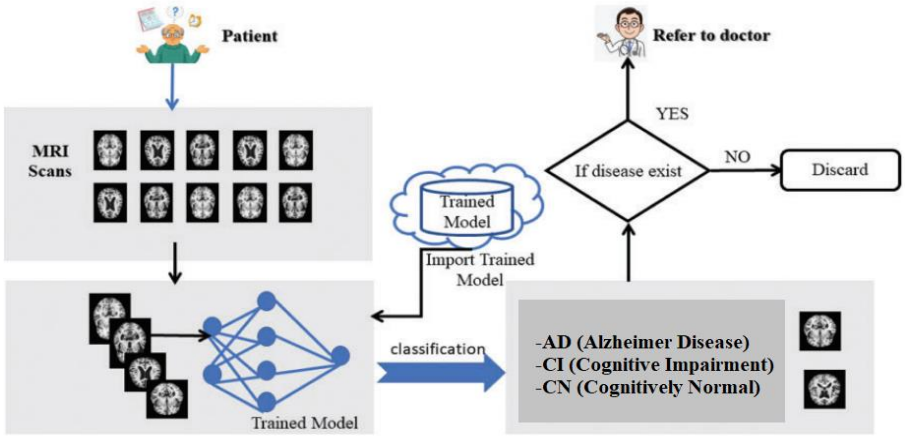


**Figure 40.** The proposed system framework.

### II.3.1. Preprocessing

In this paper, we use data augmentation as preprocessing to improve the performance and results of our neural network models by generating additional and diverse examples to train on. This task returns a rich and sufficient dataset for model training, allowing the recognition system to perform better and more accurately.

The data augmentation included rescaling the image, zooming, horizontal flipping, and brightness adjustments.

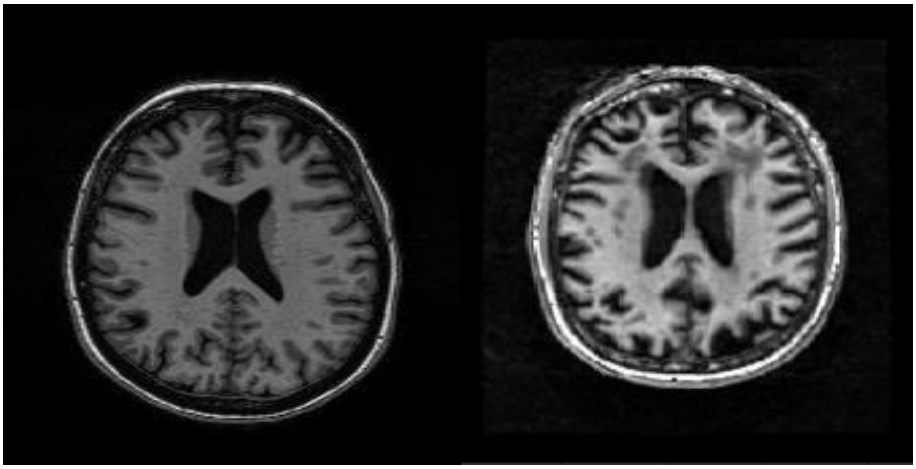

Without data augmentation with data augmentation

**Figure 41.** Example of applying data augmentation on brain MR images.

### *II.3.2. Feature extraction using deep learning*

#### II.3.2.1. VGG16 Model

VGG16 is a CNN (Convolutional Neural Network) that is widely regarded as one of the best computer vision models available today. The developers of this model evaluated the networks and enhanced the depth with a relatively small (3 3) convolution filter design, which demonstrated a considerable improvement over the prior-art setup. They increased the depth to 16-19 weight layers, resulting in around 138 million trainable parameters. VGG16 is object identification and classification method that can accurately classify 1000 photos from 1000 different categories. It is a common picture classification technique that works well with transfer learning.

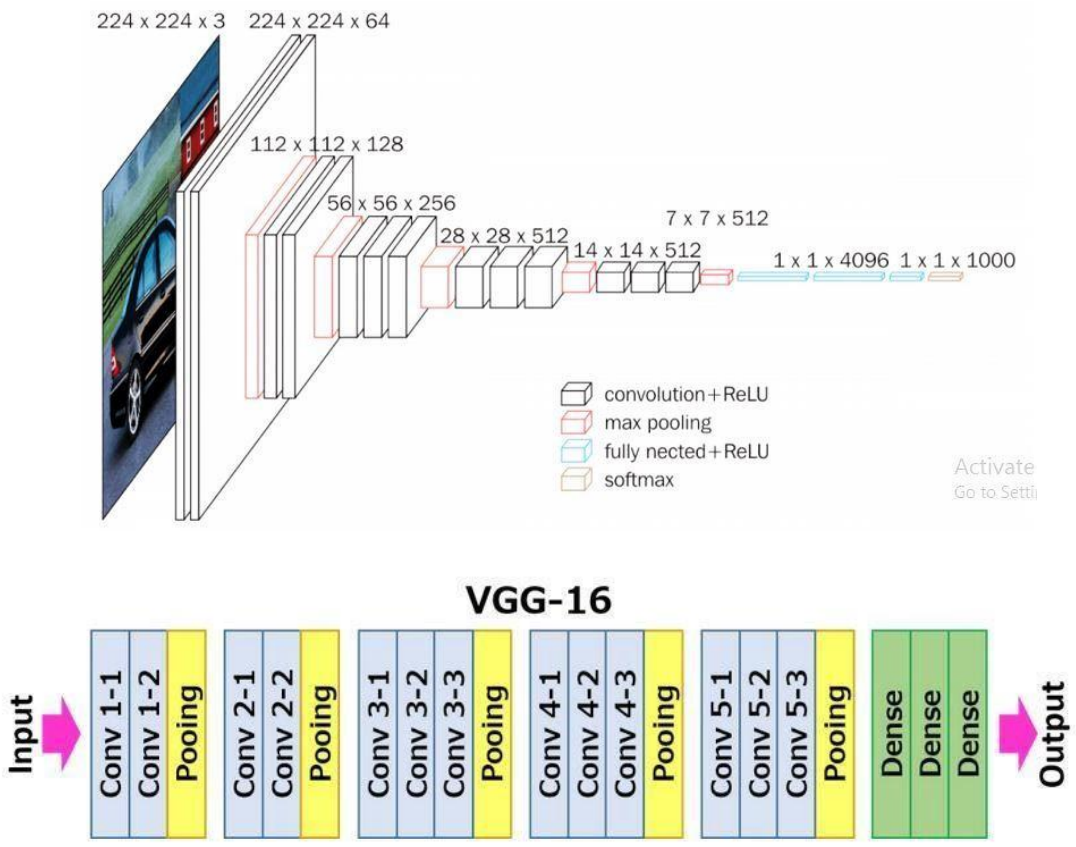


**Figure 42.** The VGG16 architecture.

The 16 in VGG16 refers to 16 layers that have weights. VGG16 has thirteen convolutional layers, five Max Pooling layers, and three dense layers, for a total of 21 layers, but only sixteen weight layers, i.e., learnable parameters layers. VGG16 takes the input tensor size as 224, 244 with 3 RGB channels. The most unique thing about VGG16 is that instead of having a large number of hyper-parameters, they focused on having convolution layers of a 3x3 filter with stride 1 and always used the same padding and max pool layer of a 2x2 filter with stride 2. The convolution and max pool layers are consistently arranged throughout the whole architecture. The Conv-1 Layer contains 64 filters; the Conv-2 Layer contains 128 filters; the Conv-3 Layer includes 256 filters, and the Conv-4 and Conv-5 Layers contain 512 filters. The three Fully-Connected (FC) layers follow a stack of convolutional layers; the first two have 4096 channels each; the third performs 1000-way ILSVRC classification and thus contains 1000 channels (one for each class). The final layer is the soft-max layer [Rohini, 2021].

### II.3.2.2. MobileNetV2 Model

The inverted residual and linear bottleneck layers in MobileNetV2 enable great accuracy and performance in mobile and embedded vision applications. The new layer builds on MobileNetV1's depth-wise separable convolutions. The MobileNetV2 network is built around this new layer, which can be customized to perform image classification and detection as well as semantic segmentation [Gonzales, 2019].

MobileNetV2 builds upon the ideas of MobileNetV1, using depth-wise separable convolution as an efficient building block. However, V2 introduces two new features to the architecture: 1) linear bottlenecks between the layers, and 2) shortcut connections between the bottlenecks. The basic structure is shown below.

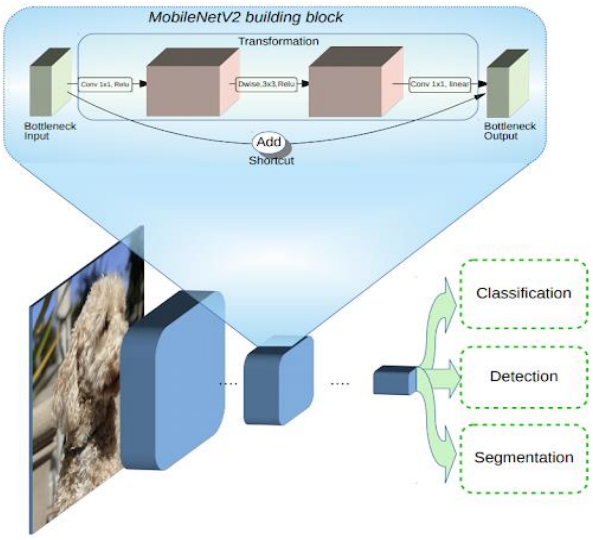

**Figure 43.** Overview of MobileNetV2 Architecture. (Blue blocks represent composite convolutional building blocks).

The intuition is that the bottlenecks encode the model's intermediate inputs and outputs while the inner layer encapsulates the model's ability to transform from lower-level concepts such as pixels to higher-level descriptors such as image categories. Finally, as with traditional residual connections, shortcuts enable faster training and better accuracy [Google AI Blog, 2018].

| Input | Operator | $t$ | $c$ | $n$ | $s$ |
|---|---|---|---|---|---|
| $224^2 \times 3$ | conv2d | - | 32 | 1 | 2 |
| $112^2 \times 32$ | bottleneck | 1 | 16 | 1 | 1 |
| $112^2 \times 16$ | bottleneck | 6 | 24 | 2 | 2 |
| $56^2 \times 24$ | bottleneck | 6 | 32 | 3 | 2 |
| $28^2 \times 32$ | bottleneck | 6 | 64 | 4 | 2 |
| $14^2 \times 64$ | bottleneck | 6 | 96 | 3 | 1 |
| $14^2 \times 96$ | bottleneck | 6 | 160 | 3 | 2 |
| $7^2 \times 160$ | bottleneck | 6 | 320 | 1 | 1 |
| $7^2 \times 320$ | conv2d 1x1 | - | 1280 | 1 | 1 |
| $7^2 \times 1280$ | avgpool 7x7 | - | - | 1 | - |
| $1 \times 1 \times 1280$ | conv2d 1x1 | - | k | - | |

**Figure 44.** MobileNetV2 architecture.

In the table above, we can see how the bottleneck blocks are arranged. t stands for the expansion rate of the channels. As we can see, they used a factor of 6. c represents the number of input channels and n represents how often the block is repeated. Lastly, s tells us whether the first repetition of a block uses a stride of 2 for the downsampling process. All in all, it's a very simple and common assembly of convolutional blocks.

The table below describes the various characteristics of our models:

**Table 4.** Comparison between the two models we used.

| Model | Size (MB) | Top-1 Accuracy | Top-5 Accuracy | Parameters | Depth | Time (ms) per inference step (CPU) | Time (ms) per inference step (GPU) |
|---|---|---|---|---|---|---|---|
| VGG16 | 528 | 71.3% | 90.1% | 138.4M | 16 | 69.5 | 4.2 |
| MobileNetV2 | 14 | 71.3% | 90.1% | 3.5M | 105 | 25.9 | 3.8 |

### II.3.3. Classification

Classification refers to a predictive modeling problem where the input data is classified as one of the predefined labeled classes, by taking on that the simplest network consists of three components: the input layer, the hidden layer, and the output layer.

The Input Layer, also known as Input Nodes, contains the inputs/information from the outside world that the model uses to learn and draw conclusions. Input nodes send data to the following layer, the Hidden layer. The hidden layer is a set of neurons that do all the computations on the input data. A neural network can have any number of hidden layers. The simplest network has a single hidden layer. The output layer is the output/conclusions of the model derived from all the computations performed. There can be single or multiple nodes in the output layer. If we have a binary classification problem, the output node is 1, but in the case of multi-class classification, the output nodes can be more than 1.

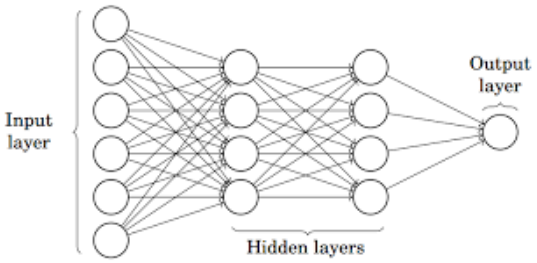


**Figure 45.** Simple neural network.

We used the SoftMax function because it is known as the activation function for multi-class classification problems where class membership is required on more than two class labels. SoftMax is a mathematical function that converts a vector of numbers into a vector of probabilities, where the probabilities of each value are proportional to the relative scale of each value in the vector.


**Figure 46.** The SoftMax function.

## CONCLUSION

In this chapter, we covered Alzheimer's disease: what it is, what its symptoms are, and the importance of detecting it early. We also discussed some of the recent studies on Alzheimer's disease classification that used deep learning approaches. We also presented the structures of our models with a mention of the features of each structure, all of which are based on the CCN framework. In the following chapter, we will report on our various results using quantitative and qualitative conversations to highlight the system's strengths and limitations.

# Chapter III: Results and discussions

## INTRODUCTION

In this final chapter, we describe the dataset we have selected to work with in terms of how we acquired it, how many cases it included, and how we applied the split function to it. Then, we look through the outcomes of our two models, and how they performed with the given data.

## III.1. DATASET DESCRIPTION

For our study, we have selected the Alzheimer's Disease Neuroimaging Initiative (ADNI) Baseline dataset (NIFTI format) which consisted of 199 instances, from Kaggle.

The dataset originally belongs to the Image & Data Archive (IDA) platform, which is owned by the Laboratory of Neuro Imaging (LONI) at the University of South California.

(ADNI) seeks to develop biomarkers of the disease and advance the understanding of AD pathophysiology, improve diagnostic methods for early detection of AD and improve the clinical trial design. Additional goals are examining the rate of progress for both cognitive impairment and Alzheimer's disease, as well as building a large repository of clinical and imaging data.

The dataset consists of 2D axial images and contains 5154 images after we applied the split function to about 80 percent for training (4123 images) and the remaining 20 percent for testing (1031 images). The dataset is divided into three classes: AD (Alzheimer's Disease), CI (Cognitive Impairment), and CN (Cognitively Normal).

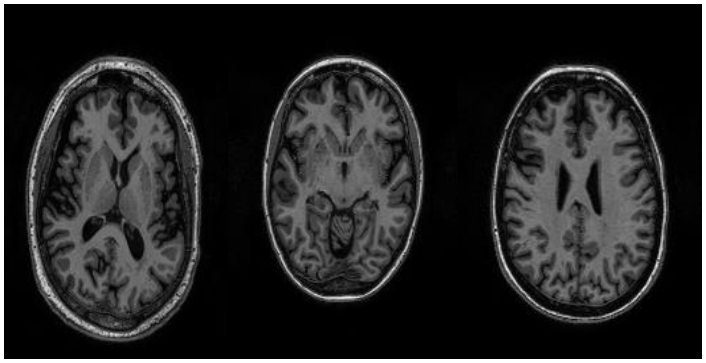

**Figure 47.** Three samples belong to the dataset one from each class.

**Table 5.** Summary for the ANDI dataset that we are using.

| | Train | | |
|---|---|---|---|
| | AD | CI | CN |
| Number of images | 899 | 2072 | 1152 |
| | Test | | |
| | AD | CI | CN |
| Number of images | 225 | 518 | 288 |

## III.2. EVALUATION METRICS

For results analysis, several performance metrics (precision, recall, f1-score, support, and accuracy) are evaluated. Accuracy is the most common way to determine the performance of a classification model. The two models give us the following results

## III.3. RESULTS

### III.3.1. Influence of preprocessing on the performance

In this experiment, we take the following model parameters:

Optimizer: Adam

Batch size: 16

Number of epochs: 20

Learning rate (L.R.) = 0.001 (default for Adam)

In this work, we use the following transforms as data augmentation:

- Rescale = 1. /255
- Horizontal Flip = True
- Brightness range = [1.0,2.0]
- Zoom range = 0.1

**Table 6.** The Influence of preprocessing on the performance of the tested models.

| | **Without data augmentation** | | **With data augmentation** | |
|---|---|---|---|---|
| Models | Training Acc. | Val. Acc. | Training Acc. | Val. Acc. |
| **VGG16** | 100.00 | **99.71** | 99.27 | 95.25 |
| **MobileNetV2** | 99.68 | **98.74** | 94.20 | 94.18 |

We can see that data augmentation does not help increase performance. As a result, we do not use data augmentation in the experiments that follow.

### III.3.2. VGG16 results

#### III.3.2.1. Influence of epoch number and batch size on VGG16 accuracy

By changing both the number of epochs and the batch size we try to find what is the best parameters that VGG16 can rely on it to give us the best results.

**Table 7.** Influence **of epoch number and batch size on VGG16 accuracy.**

| N° Epochs / Batch size | 20 | 30 | 40 | 50 |
|---|---|---|---|---|
| 16 | 99.71% | 99.61% | **99.81**% | 99.81% |
| 32 | 99.03% | 96.31% | 97.67% | 98.55% |
| 64 | 81.77% | 96.41% | 91.37% | 99.52% |

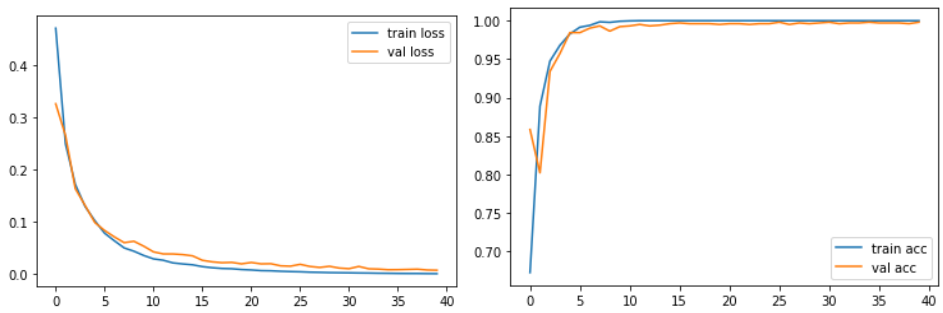


(a) (b)

***Figure 48.*** *Best results: a) Losses (training & validation). b) Accuracies (training & validation).*

The results showed that the VGG16 gave an excellent result with this parameter (number of epochs = 40 and the batch size = 16).

Also, by observing the validation accuracy curve in figure III.2. we could say that we have a very high learning rate which translates to the learning rate that controls how quickly the model is adapted to the problem.

### III.3.2.2. Influence of optimizer and learning rate on VGG16 accuracy

Now, we try to find the best optimizer alongside the best learning rate that can work with it.

**Table 8.** The Influence of epoch number and batch size on the VGG16 **accuracy**.

| Optimizer / L.R | SGD | Adam | RMSprop |
|---|---|---|---|
| 0.01 | 89.61% | 99.61% | 99.22% |
| 0.001 | 99.81% | **99.81**% | 99.52% |
| 0.0001 | 99.13% | 99.13% | 98.74% |

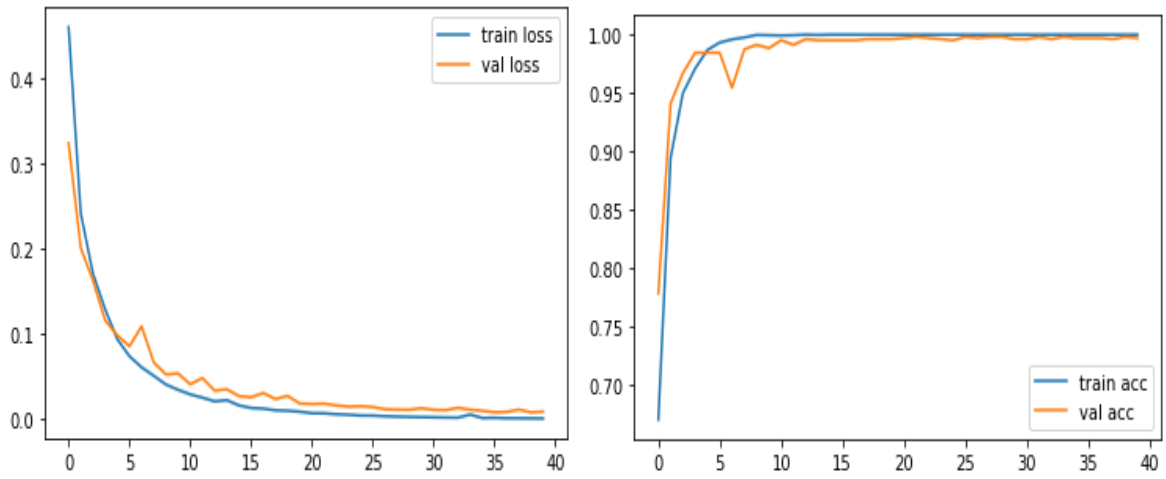


(a) (b)

**Figure 49.** Best results: a) Losses (training & validation). b) Accuracies (training & validation).

Back to the results we've got from changing between three optimizers and three values for the learning rate we see that Adam outperform both the SGD and RMSprop in this experiment, and we believe this is due to the backbone nature of Adam which managed to work well with VGG16.

### III.3.3. MobileNetV2 results

#### III.3.3.1. Influence of epoch number and batch size on the MobileNetV2 accuracy

With the same method, we applied to the VGG16, we are going to see how MobileNetV2 performs based on the different architecture that he has.

**Table 9.** The Influence of epoch number and batch size on the MobileNetV2 **accuracy**.

| N° Epochs / Batch size | 20 | 30 | 40 | 50 |
|---|---|---|---|---|
| 16 | 98.74% | 97.58% | 98.74% | 99.32% |
| 32 | 99.61% | 99.61% | **99.71**% | 99.61% |
| 64 | 99.52% | 99.61% | 99.52% | 99.61% |

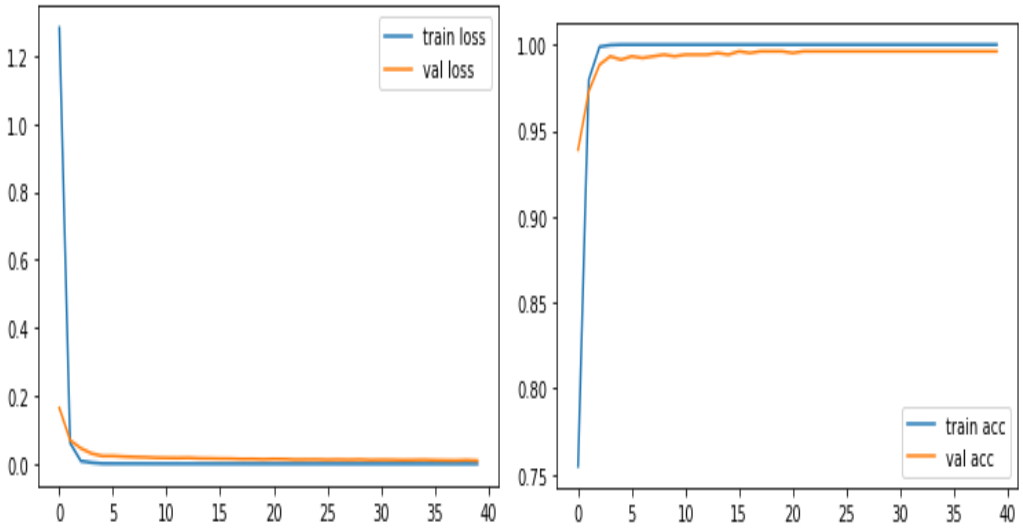


(a) (b)

**Figure 50.** Best results: a) Losses (training & validation) and b) Accuracies (training & validation).

MobileNetV2 scored his best result 99.71% with (number of epochs=40 and the batch size = 32).

Back to Figure III.4., we can see that the MobileNetV2 is more stable than the VGG16, and this is only due to how they deal with the dataset and the parameters given by us.

### III.3.3.2. Influence of optimizer and learning rate on the MobileNetV2 accuracy

By taking the best result obtained from changing the epoch number and the batch size, we try to find which optimizer with the given learning rate will perform the best.

**Table 10.** The Influence of optimizer and learning rate on the MobileNetV2 accuracy.

| Optimizer / L.R. | SGD | Adam | RMSprop |
|---|---|---|---|
| 0.01 | 96.90% | 98.74% | 99.22% |
| 0.001 | 98.55% | 99.71% | 98.64% |
| 0.0001 | 97.09% | 99.61% | **100.00**% |

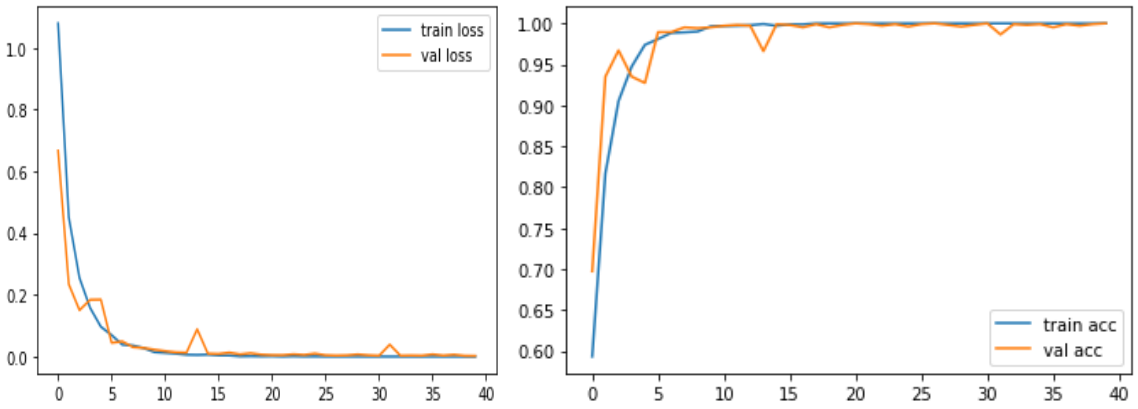


(a) (b)

**Figure 51.** Best results: a) Losses (training & validation) and b) Accuracies (training & validation).

We have 100% accuracy on the MobileNetV2 when we used RMSprop as an optimizer and 0.0001 his learning rate, other than the slight deformation observed in Figure III.5, which is due to the architecture of the model and the state of the dataset, we can say that the result obtained is excellent.

We also notice that smaller learning rates require more training epochs given the smaller changes made to the weights each update, whereas larger learning rates result in rapid changes and require fewer training epochs.

**Table 11.** Vgg16 classification report.

| | Metrics (%) | | | |
|---|---|---|---|---|
| **Datasets** | **Precision** | **Recall** | **F1-Score** | **Support** |
| **AD** | 1.00 | 0.99 | 1.00 | 225 |
| **CI** | 1.00 | 1.00 | 1.00 | 518 |
| **CN** | 1.00 | 1.00 | 1.00 | 288 |
| **Accuracy (%)** | | | **1.00** | **1031** |
| **Macro Avg** | 1.00 | 1.00 | 1.00 | 1031 |
| **Weighted Avg** | 1.00 | 1.00 | 1.00 | 1031 |

**Table 12.** MobileNetV2 classification report.

| | Metrics (%) | | | |
|---|---|---|---|---|
| **Datasets** | **Precision** | **Recall** | **F1Score** | **Support** |
| **AD** | 1.00 | 1.00 | 1.00 | 225 |
| **CI** | 1.00 | 1.00 | 1.00 | 518 |
| **CN** | 1.00 | 1.00 | 1.00 | 288 |
| **Accuracy (%)** | | | **1.00** | **1031** |
| **Macro Avg** | 1.00 | 1.00 | 1.00 | 1031 |
| **Weighted Avg** | 1.00 | 1.00 | 1.00 | 1031 |

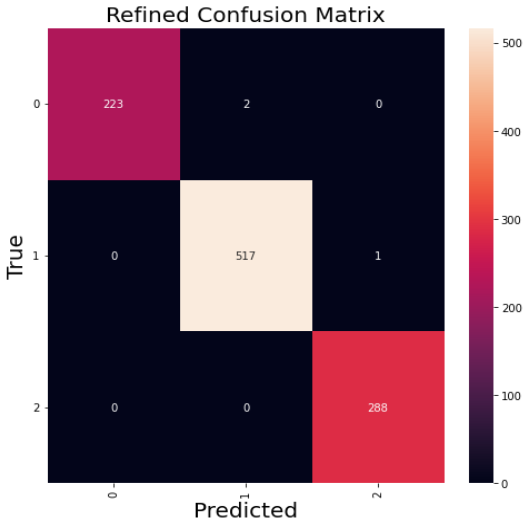


**Figure 52.** VGG16 Confusion matrix.

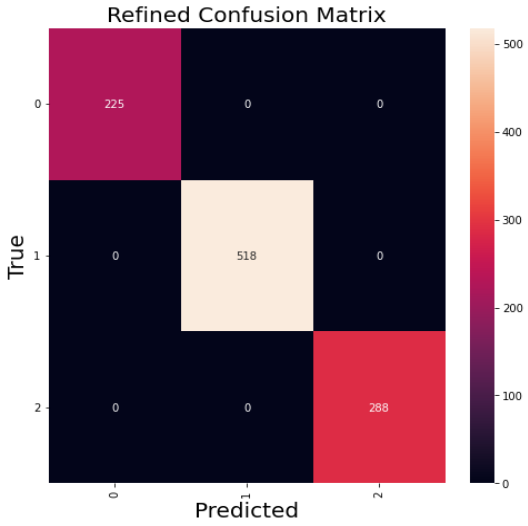


**Figure 53.** MobileNetV2 Confusion matrix.

## III.4. COMPARATIVE STUDY

In this section, we make a meaningful comparison with works that used the same dataset for Alzheimer's diagnosis. Table III.5 reports the comparison statistics.

**Table 13.** Comparison with state-of-the-art methods.

| Reference | Method | Classification | Dataset | Performance (%) | | |
|---|---|---|---|---|---|---|
| | | | | Acc. | Prec. | Sen. |
| [Salehi, 2020] | CNN | 3 | ADNI, MRI, 1512 mild, 2633 normal, 2480 AD | 99 | - | |
| [Farooq, 2017] | GoogLeNet | 4 | ADNI, MRI, 38024 images for all classes | 98.88 | 99.8 | 99.9 |
| [Raju, 2020] | 3D-CNN with SVM | 3 | ADNI, MRI, 900 images for all classes | 97.77 | - | - |
| Our work | VGG16 | 3 | ADNI, MRI, 5154 images for all classes, 899 AD, 2072 CI, 1152 CN | 99.71 | 1.00 | |
| | MobileNetV2 | 3 | | 1.00 | 1.00 | |

From Table III.9, we notice that our system performs very well with the MobileNetV2 model compared to the VGG16. Despite the number of subjects is different, but our proposed system presents a high performance in terms of accuracy and sensitivity. Through the previous table, we note that our method, which depends on VGG16 gives the best results in term of accuracy.

## CONCLUSION

The CNN technique is a great way to make predictions based on images. We try some pre-trained models using the transfer learning method to make an Alzheimer's disease classification system. Without any data augmentation or pre-processing techniques. The best result achieved by the transfer learning technique is 100% accuracy by the MobileNetV2 architecture. We need to mention too that the VGG16 model did pretty well with a 99.71% accuracy.

# General Conclusion

## General Conclusion

Our study seeks to present a deep learning system that focuses on the early diagnosis and classification of Alzheimer's disease in order to help specialists in the medical field. Transfer learning was conducted using two alternative models, VGG16 and MobileNetV2. We discovered that VGG16 and mobileNetV2 perform exceptionally well with medium-sized data, which is one of the architectures' strengths while dealing with smaller amounts of data.

To begin, the pre-trained models were trained using three-class datasets on 4123 axial MR images, which were distributed as follows: AD (899 images), CI (2072 images), and CN (1152 images). After splitting our dataset, the testing data represented 20% of it, (AD: 225 images, CI: 518 images, CN: 288 images). Each model produces a distinct result, although being relatively similar. Starting with the VGG16, which has excellent testing accuracy (99.71 %), the MobileNetV2 astonished us with a testing accuracy of 100 %.

When compared to other published research, these two models perform excellently; indeed, they are the best overall models in terms of accuracy. The highest level of state-of-the-art obtained General Conclusion accuracy.

Even if the developed system has excellent and high classification accuracy, it is still advised to seek confirmation from a medical specialist due to the chance of error.

## References


[Anderson, 1992] Anderson, D., & McNeill, G. (1992). Artificial neural networks technology. *Kaman Sciences Corporation*, *258*(6), 1-83.

[Bengio, 2017] Bengio, Y., Goodfellow, I., & Courville, A. (2017). *Deep learning* (Vol. 1). Cambridge, MA, USA: MIT Press.

[Bradley, 2000] Bradley, W. G. (2000). FUNDAMENTALS OF MRI: Part I.

[Brown, 2022] Brown, T., Morris, H., & Hossieni, A. (2022). Neurological Applications of Positron Emission Tomography Imaging in Healthcare and Research.

[Brownlee, 2022] Brownlee, J. (2022). Softmax Activation Function with Python. Retrieved 8 June 2022, from https://machinelearningmastery.com/softmax-activation-function-with-python/

[Budhiraja, 2021] Budhiraja, I., & Garg, D. (2021, December). Alzheimer's Disease Classification Using Transfer Learning. In *International Advanced Computing Conference* (pp. 73-81). Springer, Cham.

[Cardarilli, 2021] Cardarilli, G. C., Di Nunzio, L., Fazzolari, R., Giardino, D., Nannarelli, A., Re, M., & Spanò, S. (2021). A pseudo-softmax function for hardware-based high speed image classification. *Scientific reports*, *11*(1), 1-1

[Cui, 2018] Cui, R., Liu, M., & Li, G. (2018, April). Longitudinal analysis for Alzheimer's disease diagnosis using RNN. In *2018 IEEE 15th International Symposium on Biomedical Imaging (ISBI 2018)* (pp. 1398-1401). IEEE.

[Farooq, 2017] Farooq, A., Anwar, S., Awais, M., & Rehman, S. (2017, October). A deep CNN based multi-class classification of Alzheimer's disease using MRI. In *2017 IEEE International Conference on Imaging systems and techniques (IST)* (pp. 1-6). IEEE.

[FDA, 2022] Ultrasound Imaging | FDA. (2022). Retrieved 16 June 2022, from https://www.fda.gov/radiation-emitting-products/medical-imaging/ultrasound-imaging#:~:text=Ultrasound%20imaging%20(sonography)%20uses%20high,flowing%20through%20the%20blood%20vessels.

[Gershenson, 2003] Gershenson, C. (2003). Artificial neural networks for beginners. *arXiv preprint cs/0308031*.

[Ghazal, 2022] Ghazal, T. M., & F Issa, G. (2022). Alzheimer disease detection empowered with transfer learning. *Computers, Materials & Continua*, *70*(3), 5005-5019.

[Ginat, 2014] Ginat, D. T., & Gupta, R. (2014). Advances in computed tomography imaging technology. *Annual review of biomedical engineering*, *16*, 431-453.

[Gonzales, 2019] Gonzales, L. (2019, November 3). A look at mobilenetv2: Inverted residuals and linear bottlenecks. Medium. Retrieved June 24, 2022, from https://medium.com/@luis_gonzales/a-look-at-mobilenetv2-inverted-residuals-and-linear-bottlenecks-d49f85c12423.

[Goodfellow, 2016] Goodfellow, I., Bengio, Y., & Courville, A. (2016). *Deep learning*. MIT press.

[Google AI Blog, 2018] MobileNetV2: The next generation of on-device computer vision networks. Google AI Blog. (2018, April 3). Retrieved June 24, 2022, from https://ai.googleblog.com/2018/04/mobilenetv2-next-generation-of-on.html

[Gu, 2018] Gu, J., Wang, Z., Kuen, J., Ma, L., Shahroudy, A., Shuai, B., ... & Chen, T. (2018). Recent advances in convolutional neural networks. *Pattern Recognition*, *77*, 354-377.

[Guo, 2020] Guo, Y., Li, Y., Wang, L., & Rosing, T. (2020, April). Adafilter: Adaptive filter fine-tuning for deep transfer learning. In *Proceedings of the AAAI Conference on Artificial Intelligence* (Vol. 34, No. 04, pp. 4060-4066).

[Hamet, 2017] Hamet, P., & Tremblay, J. (2017). Artificial intelligence in medicine. *Metabolism*, *69*, S36-S40.

[Hecht-Nielsen,1992] Hecht-Nielsen, R. (1992). Theory of the backpropagation neural network. In *Neural networks for perception* (pp. 65-93). Academic Press.

[Helaly, 2021] Helaly, H. A., Badawy, M., & Haikal, A. Y. (2021). Deep learning approach for early detection of Alzheimer's disease. *Cognitive computation*, 1-17.

[Hochreiter, 1997] Hochreiter, S., & Schmidhuber, J. (1997). Long short-term memory. *Neural computation*, *9*(8), 1735-1780.

[Hon, 2017] Hon, M., & Khan, N. M. (2017, November). Towards Alzheimer's disease classification through transfer learning. In *2017 IEEE International conference on bioinformatics and biomedicine (BIBM)* (pp. 1166-1169). IEEE.

[Howard, 2017] Howard, A. G., Zhu, M., Chen, B., Kalenichenko, D., Wang, W., Weyand, T., ... & Adam, H. (2017). Mobilenets: Efficient convolutional neural networks for mobile vision applications. arXiv preprint arXiv:1704.04861.

[Jaakkola, 2019] Jaakkola, H., Henno, J., Mäkelä, J., & Thalheim, B. (2019, May). Artificial intelligence yesterday, today and tomorrow. In *2019 42nd International Convention on Information and Communication Technology, Electronics and Microelectronics (MIPRO)* (pp. 860-867). IEEE.

[Kaul, 2020] Kaul, V., Enslin, S., & Gross, S. A. (2020). History of artificial intelligence in medicine. *Gastrointestinal endoscopy*, *92*(4), 807-812.

[Ke, 2018] Ke, Q., Liu, J., Bennamoun, M., An, S., Sohel, F., & Boussaid, F. (2018). Computer vision for human–machine interaction. In *Computer Vision for Assistive Healthcare* (pp. 127-145). Academic Press.

[Khan, 2020] Khan, A., Sohail, A., Zahoora, U., & Qureshi, A. S. (2020). A survey of the recent architectures of deep convolutional neural networks. *Artificial intelligence review*, *53*(8), 5455-5516.

[Kim, 2021] Kim, B., Yuvaraj, N., Sri Preethaa, K. R., & Arun Pandian, R. (2021). Surface crack detection using deep learning with shallow CNN architecture for enhanced computation. *Neural Computing and Applications*, *33*(15), 9289-9305.

[Krizhevsky, 2012] Krizhevsky, A., Sutskever, I., & Hinton, G. E. (2012). Imagenet classification with deep convolutional neural networks. *Advances in neural information processing systems*, *25*.

[Kumar, 2022] Kumar, A. (2022, April 12). Different types of CNN Architectures explained: Examples. Retrieved June 7, 2022, from https://vitalflux.com/different-types-of-cnn-architectures-explained-examples/#:~:text=ZF%20Net%20CNN%20architecture%20consists,before%20the%20fully%20connected%20output.

[Kundaram, 2021] Kundaram, S. S., & Pathak, K. C. (2021). Deep learning-based Alzheimer disease detection. In *Proceedings of the fourth international conference on microelectronics, computing and communication systems* (pp. 587-597). Springer, Singapore.

[LeCun, 1995] Le Cun, Y. ea (1995). Handwritten digit recognition with a back propagation network. In *International Conference on Artificial Neural Networks* (pp. 53-60).

[LeCun, 1998] LeCun, Y., Bottou, L., Bengio, Y., & Haffner, P. (1998). Gradient-based learning applied to document recognition. *Proceedings of the IEEE*, *86*(11), 2278-2324.

[LeCun, 2015] LeCun, Y., Bengio, Y., & Hinton, G. (2015). Deep learning. *nature*, *521*(7553), 436-444.

[Maqsood, 2019]Maqsood, M., Nazir, F., Khan, U., Aadil, F., Jamal, H., Mehmood, I., & Song, O. Y. (2019). Transfer learning assisted classification and detection of Alzheimer's disease stages using 3D MRI scans. *Sensors*, *19*(11), 2645.

[Mathew, 2020] Mathew, A., Amudha, P., & Sivakumari, S. (2020, February). Deep learning techniques: an overview. In *International conference on advanced machine learning technologies and applications* (pp. 599-608). Springer, Singapore.

[Mazonakis, 2016] Mazonakis, M., & Damilakis, J. (2016). Computed tomography: What and how does it measure?. *European journal of radiology*, *85*(8), 1499-1504.

[McCarthy, 2014] McCarthy, J. (2004). What is artificial intelligence. *URL: http://www-formal. stanford. edu/jmc/whatisai. html*.

[Michele, 2019] Michele, A., Colin, V., & Santika, D. D. (2019). Mobilenet convolutional neural networks and support vector machines for palmprint recognition. *Procedia Computer Science*, *157*, 110-117.

[Montavon, 2012] Montavon, G., & Müller, K. R. (2012). Deep Boltzmann machines and the centering trick. In *Neural networks: tricks of the trade* (pp. 621-637). Springer, Berlin, Heidelberg.

[Nam, 2018] Nam Nam, S., Park, H., Seo, C., & Choi, D. (2018). Forged signature distinction using convolutional neural network for feature extraction. *Applied Sciences*, *8*(2), 153.

[NHS, 2022] NHS. (n.d.). *Endoscopy*. NHS . Retrieved June 16, 2022, from https://www.nhs.uk/conditions/endoscopy/#:~:text=An%20endoscopy%20is%20a%20test,endoscopy%20unit%20in%20a%20hospital.

[Pan, 2009] Pan, S. J., & Yang, Q. (2009). A survey on transfer learning. *IEEE Transactions on knowledge and data engineering*, *22*(10), 1345-1359.

[Prasad,2022] Prasad, A. (2022). Why Retinal Imaging is an Important Part of Your Eye Exam. Retrieved 16 June 2022, from https://okeyecare.com/why-retinal-imaging-is-an-important-part-of-your-eye-exam/#:~:text=Retinal%20imaging%20is%20a%20non,blood%20vessels%20inside%20the%20eye.

[Raju, 2020] Raju, M., Gopi, V. P., Anitha, V. S., & Wahid, K. A. (2020). Multi-class diagnosis of Alzheimer's disease using cascaded three dimensional-convolutional neural network. *Physical and Engineering Sciences in Medicine*, *43*(4), 1219-1228.

[Rath, 2022] Rath, S. (2022). Convolutional Neural Network Architectures and Variants - DebuggerCafe. Retrieved 4 June 2022, from https://debuggercafe.com/convolutional-neural-network-architectures-and-variants/

[Rohini, 2021] Rohini, G. (2021, September 23). Everything you need to know about VGG16. Medium. Retrieved June 24, 2022, from https://medium.com/@mygreatlearning/everything-you-need-to-know-about-vgg16-7315defb5918

[RSNA, 2022] Radiological Society of North America (RSNA) and American College of Radiology (ACR). (2022, April 15). *Elastography*. Radiologyinfo.org. Retrieved June 16, 2022, from https://www.radiologyinfo.org/en/info/elastography#:~:text=Elastography%20is%20a%20non%2Dinvasive,frequency%20vibrations%20into%20the%20liver.

[Salehi, 2020] Salehi, A. W., Baglat, P., Sharma, B. B., Gupta, G., & Upadhya, A. (2020, September). A CNN model: earlier diagnosis and classification of Alzheimer disease using MRI. In *2020 International Conference on Smart Electronics and Communication (ICOSEC)* (pp. 156-161). IEEE.

[Sandler, 2018] Sandler, M., Howard, A., Zhu, M., Zhmoginov, A., & Chen, L. C. (2018). Mobilenetv2: Inverted residuals and linear bottlenecks. In *Proceedings of the IEEE conference on computer vision and pattern recognition* (pp. 4510-4520).

[Sarker, 2021] Sarker, I. H. (2021). Deep learning: a comprehensive overview on techniques, taxonomy, applications and research directions. *SN Computer Science*, *2*(6), 1-20.

[Simonyan, 2014] Simonyan, K., & Zisserman, A. (2014). Very deep convolutional networks for large-scale image recognition. *arXiv preprint arXiv:1409.1556*.

[Suryanarayana, 1998] Suryanarayana, C., & Norton, M. G. (1998). X-rays and Diffraction. In *X-ray Diffraction* (pp. 3-19). Springer, Boston, MA.

[Szegedy, 2015] Szegedy, C., Liu, W., Jia, Y., Sermanet, P., Reed, S., Anguelov, D., ... & Rabinovich, A. (2015). Going deeper with convolutions. In *Proceedings of the IEEE conference on computer vision and pattern recognition* (pp. 1-9).

[Tajbakhsh, 2016] Tajbakhsh, N., Shin, J. Y., Gurudu, S. R., Hurst, R. T., Kendall, C. B., Gotway, M. B., & Liang, J. (2016). Convolutional neural networks for medical image analysis: Full training or fine tuning?. *IEEE transactions on medical imaging*, *35*(5), 1299-1312.

[Varshney, 2020] Varshney, P. (2020). VGGNet-16 Architecture: A Complete Guide. Retrieved 12 June 2022, from https://www.kaggle.com/code/blurredmachine/vggnet-16-architecture-a-complete-guide/notebook

[Walczak, 2018] Walczak, S. (2018). Artificial neural networks. In *Encyclopedia of Information Science and Technology, Fourth Edition* (pp. 120-131). IGI Global.

[Wang, 2019] Wang, F., & Preininger, A. (2019). AI in health: state of the art, challenges, and future directions. *Yearbook of medical informatics*, *28*(01), 016-026.

[Yingge, 2020] Yingge, H., Ali, I., & Lee, K. Y. (2020, February). Deep neural networks on chip-A survey. In *2020 IEEE International Conference on Big Data and Smart Computing (BigComp)* (pp. 589-592). IEEE.

[Yosinski, 2014] Yosinski, J., Clune, J., Bengio, Y., & Lipson, H. (2014). How transferable are features in deep neural networks?. *Advances in neural information processing systems*, *27*

## Abstract:

This dissertation focuses on Alzheimer's disease diagnosis using deep learning techniques applied to MRI images.

With the rapid advancements and changes in technology and AI techniques, they could aid in diagnosis and classification while posing no significant risks by utilizing existing MRI image data. Although there are no working treatments yet, only medicines that can help slow the progression of the disease, early detection and classification could help choose the best treatment plan.

We chose the transfer learning method, employing two well-known pre-trained CNN models (VGG16 & MobileNetV2). The experimental results show that our proposed approach outperforms other approaches and methods in terms of accuracy, achieving 99.71% with VGG16 and 100.0% with MobileNetV2.

## ملخص:

تركز هذه الرسالة على تشخيص مرض الزهايمر باستخدام تقنيات التعلم العميق المطبقة على صور التصوير بالرنين المغناطيسي

مع التطورات والتغييرات السريعة في التكنولوجيا وتقنيات الذكاء الاصطناعي، يمكن أن تساعد في التشخيص والتصنيف بينما لا تشكل أي مخاطر كبيرة من خلال استخدام بيانات صور التصوير بالرنين المغناطيسي الموجودة. على الرغم من عدم وجود علاجات فعالة حتى الآن، إلا الأدوية التي يمكن أن تساعد في إبطاء تقدم المرض، يمكن أن يساعد الاكتشاف المبكر والتصنيف في اختيار أفضل خطة علاج.

لقد اخترنا طريقة تعلم النقل، باستخدام نموذجين معروفين مسبقًا من CNN (VGG16 وMobileNetV2). أظهرت النتائج التجريبية أن نهجنا المقترح يتفوق على الأساليب والطرق الأخرى من حيث الدقة والثبات، حيث حقق 99.71٪ مع VGG16 و100.0٪ مع MobileNetV2.